MASTERARBEIT | MASTER'S THESIS

Titel | Title

Species of *Prospero autumnale* complex in Crete

verfasst von | submitted by

Konstantinos Kotsampas

angestrebter akademischer Grad | in partial fulfilment of the requirements for the degree of

Master of Science (MSc)

Wien | Vienna, 2025

Studienkennzahl lt. Studienblatt | Degree programme code as it appears on the student record sheet:	UA 066 832
Studienrichtung lt. Studienblatt | Degree programme as it appears on the student record sheet:	Masterstudium Botany
Betreut von | Supervisor:	Univ.-Prof. Mag. Dr. Hanna Schneeweiss Privatdoz.

Acknowledgments

I would like to express my sincere gratitude to all those who supported me throughout the journey of my master's thesis.

First and foremost, I would like to thank my supervisor, Professor Dr. Hanna Weiss-Schneeweiss, for her constant guidance, constructive feedback, and encouragement at every stage of this thesis. I am especially grateful for the opportunity to collaborate with her and help shape the direction of the research. A process that kept me fully engaged and motivated, and taught me important principles of scientific ethics and progress.

I am also deeply grateful to the members of the Plant Evolutionary Cytogenetics research group for their continuous support during the laboratory work. In particular, I thank our beloved lab technician, Rebecca Schmidt, for her contribution to flow cytometry measurements and for her extensive guidance during the phylogenetic analyses. My sincere thanks also go to Rosemarie Benthen for her active guidance in fluorescence *in situ* hybridization analysis, as well as her help in solving every challenge that arose and for her always constructive discussions. I would also like to thank Laura Pflügl, my fellow study companion, for sharing this academic journey with me, from practical concerns to scientific insights, and Vildana Kapetanovic, whose uplifting presence and encouragement helped me stay grounded and motivated throughout the year.

The collection trip would not have been possible without the generous help of my dear friends Dimitra, Kali and Marios. Their selfless support made the fieldwork not only feasible, but also truly unforgettable.

Lastly, I extend my thanks to the entire Division of Systematic and Evolutionary Botany at the University of Vienna for providing a stimulating and supportive academic environment. The easy access to resources and the welcoming atmosphere created by everyone I encountered during my work made the overall experience really enjoyable.

Thank you all.

Table of Contents

Introduction

Prospero autumnale complex

Taxonomic treatments and evolutionary inferences are traditionally based on morphological characters often implemented with cytological and genetic analyses. Nevertheless, depending on the evolutionary trajectories of each plant group, resolving the intricate relationships between species can be challenging. Many species encompass more than one cytotype, identified based on significant genomic and chromosomal differences. Distinct cytotypes are usually characterized by unique combinations of basic chromosome numbers and/or ploidy levels, genome sizes, and the number and localization of rDNA and satellite DNA loci, as well as other repetitive DNA regions (Weiss-Schneeweiss et al., 2013). However, such biological entities do not necessarily represent discrete taxonomic units. Investigating plant groups that are defined by complex and variable cytological character combinations can provide insight into their evolutionary history and establishment, and most importantly, the role of chromosomal change in diversification and speciation. *Prospero autumnale* (L). Speta complex is an excellent system in which to address such questions.

The genus *Prospero* Salisb. belongs to the family Asparagaceae, subfamily Scilloideae (formerly Hyacinthaceae). It represents a morphologically and cytologically distinct lineage that was historically treated within the broadly defined genus *Scilla* L., until taxonomic revision supported by molecular, morphological and karyological evidence, clearly demonstrated that it deserves a status of a separate genus (Speta 1982, 1998; Govaerts, 2015). Members of the genus are primarily autumn flowering and are characterized by hysteranthous leaf development (leaves appearing after flowering), the absence of bracts and prophylls and the lack of elaiosome on the seeds, in contrast to their closest relative *Scilla* L. (Speta, 1986). However, some exceptions to the presence of some of the characters were reported, like the presence of small bracts in plants belonging to three *Prospero* Salisb. cytotypes (Ainsworth, 1980). Two additional exceptions were reported from two newly described species from Southeastern Anatolia in Turkey: *Prospero seisumsianum* (Rukšāns & Zetterl.) Yıldırım which exhibits spring leaf emergence and the spring flowering synanthous *Prospero cudidaghense* Firat & Yıldırım, highlighting the potential plasticity within the genus. Comparative analyses of all taxa in the genus allowed to distinguish two species: *Prospero obtusifolium* (Poir.) Speta and

Prospero hanburyi (Baker) Speta, as well as one species complex of *Prospero autumnale* (Figure 1). The latter is the most taxonomically and cytologically complex representative of the genus with many local segregates described within its distribution range that extends from southern England and the Mediterranean basin to the Caucasus and northern Iraq (Speta, 1982). These taxa are often not defined by clear morphological differences, complicating the delimitation of species within the group (Vaughan et al., 1997).

Prospero autumnale s.l. is a bulbous perennial producing bulbs that can be up to 4.5 cm in diameter. Each individual bulb can produce up to six inflorescences per season, with individual scapes being 4–25 cm at anthesis and having simple racemes of 4–40 flowers. In northwestern Europe, flowering typically begins in July or August and extends into early September, whereas in southern populations, flowering occurs later and continues throughout the autumn. Floral anthesis within a raceme spans 5 to 14 days, depending on the season and flower count. The flowers possess six free, lanceolate perianth segments (4–7.5 mm) with a prominent midrib and are supported by ascending pedicels (2–5 mm). Anthers are attached on 3–5 mm filaments and dehisce shortly after the flowers open. Floral coloration is variable, ranging from pink to lilac with a darker midrib and purple anthers, to white tepals with yellow anthers. The trilocular ovary, white or blue in color, bears a centrally positioned style, and matures into an ellipsoid capsule (~2mm in diameter), typically containing up to two seeds per locule. The leaves are linear (4–20cm × 1–5mm) and exhibit geographically variable senescence, typically withering by April in southern populations, while in northern populations they may persist year-round. Reproduction is predominantly sexual, occurring through seeds. Most individuals are outcrossers, though limited self-fertilization can result in seed set. Vegetative reproduction is rare, having only been observed in a few individuals among several hundred examined and usually is a response to original bulb wounding (Ainsworth, 1980). Despite the wide range of morphological traits observed, all the described taxa within the group fall within the phenotypic boundaries of *Prospero autumnale* s.l., suggesting that *Prospero autumnale* might represent a species complex.

The complexity of the variable morphology is accompanied by the existence of multiple cytological races (Ainsworth, 1980; Vaughan, 1997) suggesting the dynamic genomic nature of this species. Multiple and distinct diploid and polyploid cytotypes are each characterized by specific sets of genomic characters. Notably, their geographically structured distribution suggests a non-random and recurrent emergence of distinct evolutionary entities/cytotypes, varying in their capacity for establishment and range expansion. This extensive chromosomal

diversity, however, is not accompanied by structured morphological differentiation. The full extent of cytological diversity within the complex still remains unknown, particularly in the eastern part of its distribution range, where detailed cytological studies are lacking. Analyses of limited material from these regions indicate strong potential for the discovery of novel cytotypes, which may be important for understanding the evolutionary history and diversification of the complex (Ebert et al., 1996; Weiss-Schneeweiss, unpubl.).

Diploid cytotypes

The distribution of the whole *Prospero autumnale* complex is circum-Mediterranean. Previous studies have identified four distinct basic diploid cytotypes, with base chromosome numbers of x = 5, 6 or 7, referred to as B^5B^5, B^6B^6, AA and B^7B^7, the latter two both based on x = 7 (Jang et al., 2013). Each of these cytotypes has unique geographical distribution. B^7B^7 is the most widespread cytotype and is found across the whole distribution range of the species complex. Its distribution overlaps with cytotype AA on the Iberian Peninsula and in northern Morocco, and with cytotype B^6B^6 on the island of Crete. In some localities, these cytotypes have even been reported to co-occur within the same populations (Taylor, 1997). In contrast, cytotype B^5B^5 is restricted to Libya, where B^7B^7 has not yet been recorded (Jang et al., 2013).

Each of the diploid cytotypes possess distinct combination of chromosome number, karyotype morphology, nuclear DNA amount as well as the localization of the 35S and 5S rDNA loci and the pericentric satellite DNA *PaB6* (Jang et al., 2013; Emadzade et al., 2014). The phylogenetic and cytogenetic data suggest that ancestral karyotype possessed x = 7. It has been hypothesized that this ancestral karyotype gave rise to all extant cytotypes (Figure 2). AA cytotype (x = 7) was hypothesized to have evolved via the loss of 5S rDNA from chromosome 1 accompanied by the increase of genome size, whereas B^7B^7 cytotype (also x = 7) via the loss of 5S rDNA from chromosome 2. The latter cytotype has been found to comprise two further types, Type I and II, differing in the presence of the duplicated or single 5S rDNA locus in chromosome 1 and the genome size. The B^6B^6 cytotype was inferred to have evolved via the descending dysploidy from base chromosome number x = 7 via the fusion of chromosomes 6 and 7, resulting in a large, easily distinguishable, sub-metacentric chromosome referred to as F^1(6-7). The genome size of this cytotype was significantly higher and Nucleolus Organizer Region (NOR) has been found to be located in a more median position in chromosome 3. Additionally, in some individuals, translocations of one or both NORs have also been documented. The last distinct cytotype, B^5B^5, was hypothesized to have originated from within B^7B^7 cytotype via independent descending dysploidy event involving the two putative fusion events involving

chromosomes 1 and 3 and either chromosome 6 or 7, resulting in two large sub-metacentric chromosomes, F^2(1-6/7) and F^3(3-6/7) (Jang et al., 2013).

Although the sets of genomic characters distinguishing cytotypes are consistent, multiple individuals have been reported that deviate from the standard karyological profile associated with their respective cytotypes. This deviation is particularly evident in the B^7B^7 cytotype, which is the most widespread and, therefore, more likely to have accumulated additional variation over time (Taylor, 1997). With respect to genome size, several individuals from this cytotype have been documented with significantly elevated DNA content (approximately 5.5–7.5 pg/1C), particularly in the western part of its distribution range, including populations from Malta and Corsica (Ebert et al., 1996; Weiss-Schneeweiss et al., unpubl.). Another population with increased genome size, accompanied by a distinct karyotypic morphology, has been reported from the Kemer and Findikpinar localities in Turkey, with genome sizes of 4.86 pg/1C

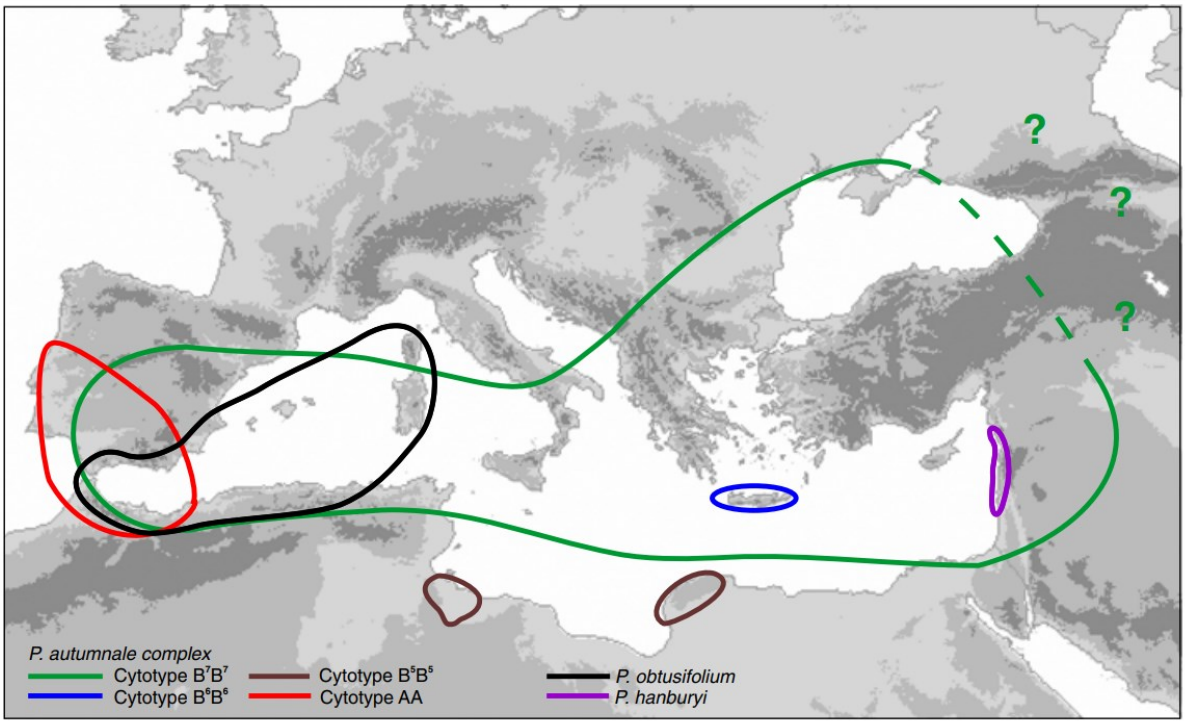

Figure 1. Geographic distribution of diploid species and cytotypes of the genus *Prospero* Salisb. Dashed line in the eastern range of distribution of cytotype $B^7B^7$and question marks indicate incomplete information on the distribution of this cytotype (Jang et al., 2013).

and 6.56 pg/1C, respectively. Both karyotypes exhibited presence of a conspicuously large metacentric chromosome resembling that of the B^6B^6 cytotype despite base chromosome number of x = 7. Despite gross similarities, these karyotypes also display notable genomic deviations from the typical B^7B^7 profile (Ebert et al., 1996).

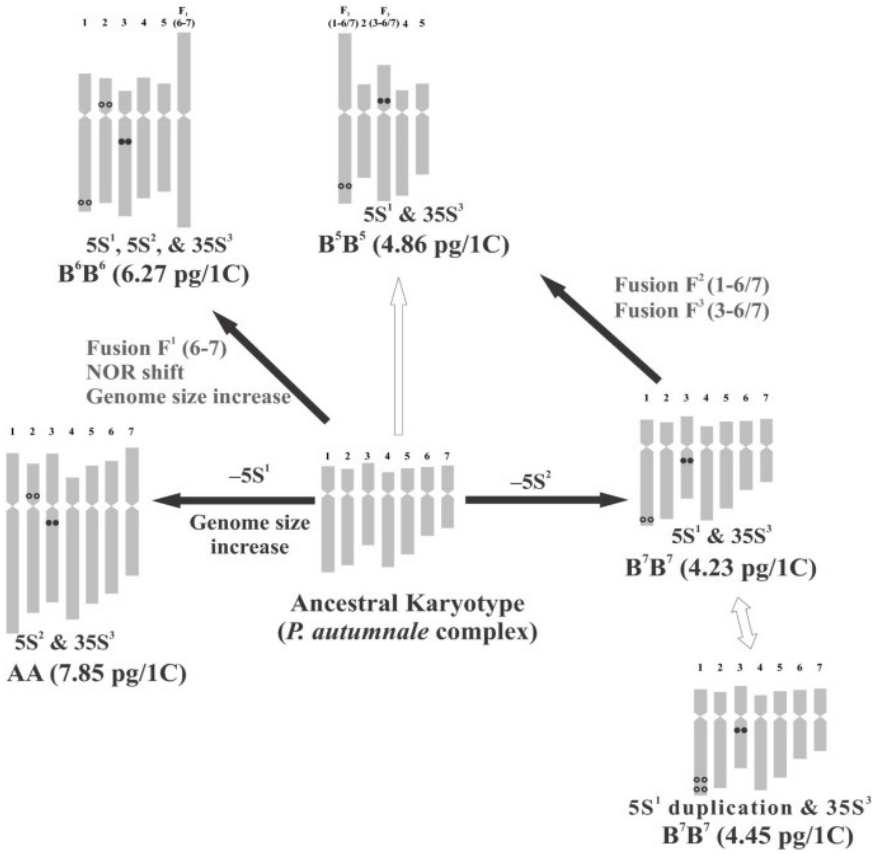

Figure 2. Current hypothesis on genome evolution of diploid cytotypes of *Prospero autumnale* complex. The model is based on karyotype morphology, rDNA loci localization, and genome size interpreted in a phylogenetic context. 5S rDNA loci are indicated as open circles, and 35S rDNA loci as closed circles. Black arrows indicate most parsimonious hypotheses, empty arrows indicate alternatives (Jang et al., 2013).

Polyploid cytotypes

In addition to the presence of well-established diploid cytotypes, multiple polyploids have independently emerged, become established, and subsequently spread beyond their areas of origin (Jang et al., 2018a). Autopolyploids as well as allopolyploids have been found across the *Prospero autumnale* cytotypes, encompassing mostly tetraploids and hexaploids, but also higher ploidy levels up to 20*x*. For many of the polyploids the parental cytotypes have been identified (Jang et al., 2018a). Nevertheless, morphological similarity to their diploid progenitors, the varying levels of intrapopulational uniformity and distinctiveness of morphological character sets raises the question whether these polyploids represent intra-specific chromosomal races or closely related, but separate species. To date, autopolyploids have only been identified in B^7B^7 lineage, and were inferred to have formed at least twice from the two different types of B^7B^7 diploids (Jang et al., 2018a). Notably, B^7 autopolyploids have never been reported on the island of Crete. Autopolyploids are the only known cytotype of

Prospero autumnale complex occurring in England and France, dominant in Italy and common in the Balkans as well as the Iberian Peninsula (Ainsworth, 1980; Ebert et al., 1996; Vaughan et al., 1996).

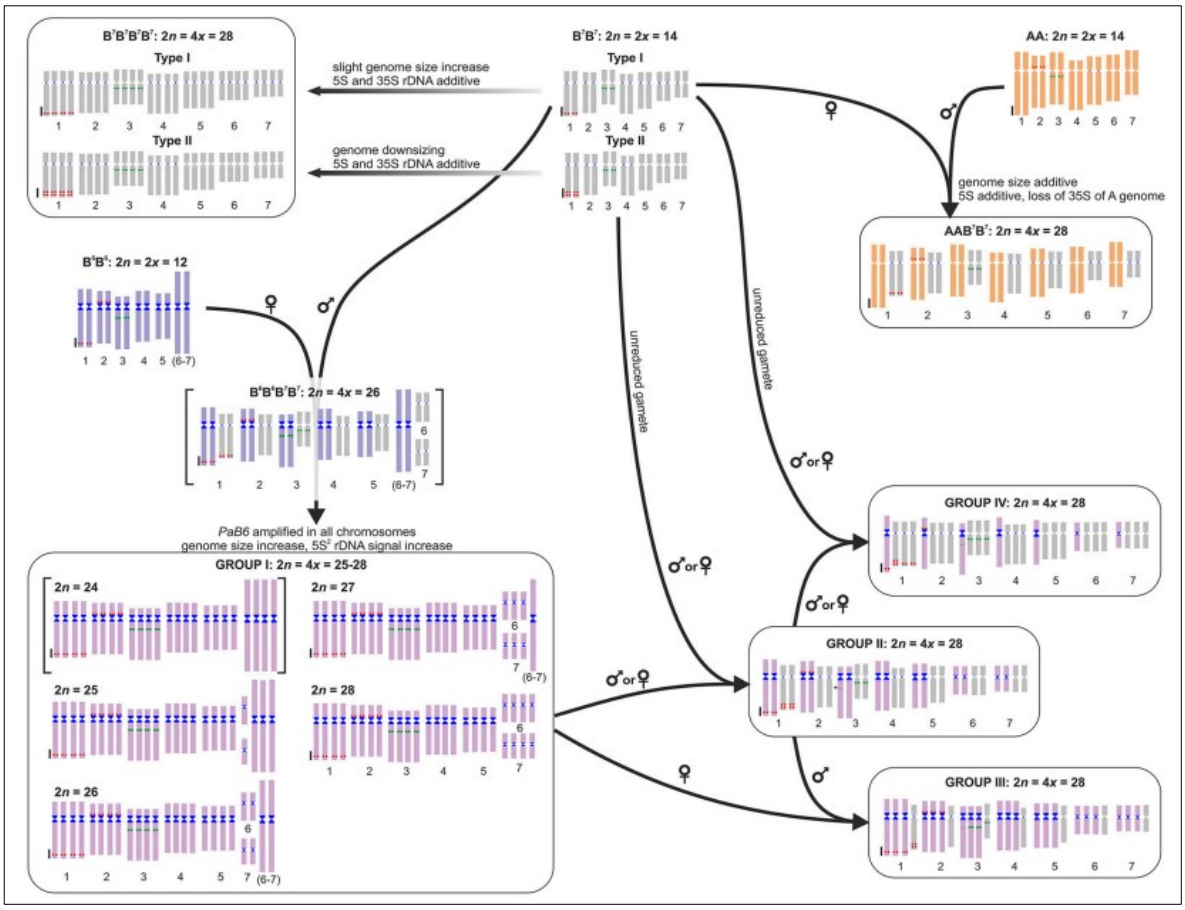

Figure 3. Model of the origin and evolution of $B^6B^6B^7B^7$ allopolyploids of *Prospero autumnale* complex. Diploid genomes represented by standard idiograms, with mapped 5S rDNA (red), 35S rDNA (green), and satellite DNA *PaB6* (blue) signals. The $B^6B^6B^7B^7$ allotetraploid with $2n = 4x = 24$ is inferred but not found in nature (in square brackets). Parental subgenomes of Group I plants cannot be identified using GISH and are thus indicated by a single unique color. Group I chromosomes can be tracked in Groups II, III, and IV. Arrows indicate directions of crosses; inferred maternal and paternal parents are indicated (Jang et al., 2018a).

The geographical proximity of some of the diploid cytotypes has also resulted in numerous hybridization events and both diploid and polyploid hybrid (allopolyploids) lineages were formed, increasing the number of established cytotypes within the complex. In particular, the derived AAB^7B^7 ($2n = 4x = 28$) allotetraploid cytotype is meiotically stable and characterized by slightly higher genome size compared to the expected additive value of the two parental lineages, an additive numbers of 5S rDNA loci and the loss of 35S rDNA locus of the A parental genome (Jang et al., 2018a).

The formation of $B^6B^6B^7B^7$ allotetraploids that has occurred on the island of Crete, is the most complex case of polyploidization within the group. These polyploids exhibit a range of chromosome numbers ($2n = 4x = 25$-28) but are genetically balanced due to the presence of a

fusion chromosome F^1(6-7) that allows for the balanced meiotic chromosome segregation (Figures 3,4). Additionally, genome homogenization towards maternal B^6B^6 parent, numerical convergence and nested cycles of hybridization among the original allotetraploids and their diploid progenitors have resulted in four distinct groups that possess distinct genomic features and are easily identifiable using combination of cytogenetic characters. These encompass number and localization of 5S and 35S rDNA loci, as well as pericentric loci of satellite DNA *PaB6* (Jang et al., 2013; Emadzade et al., 2014) which allow to trace the genomic composition and origin of allotetraploids. Changes in copy number, loci number, and the distribution of repetitive DNA sequences, as well as changes of genome sizes, are consistent markers allowing for identification of all four allotetraploid groups on Crete (Jang et al., 2018a).

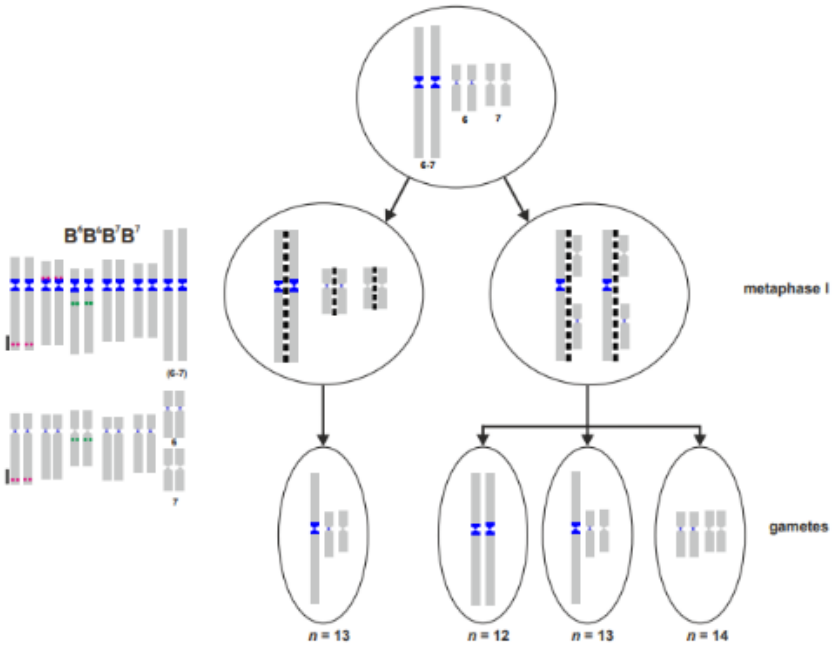

Figure 4. Meiotic pairing behavior resulting in numerical variation in $B^6B^6B^7B^7$allotetraploids of Group I. Left: *in silico* karyotype of $B^6B^6B^7B^7$allotetraploid, $2n = 4x = 26$. Right: only pairing and segregation patterns of free chromosomes 6, 7 and fusion chromosome F^1 (6-7) are indicated, since these lead to numerical variation in meiotic products. From top to bottom: set of free chromosomes 6, 7 and a fusion chromosome F^1(6-7); two modes of pairing in meiosis I; segregation of these chromosomes in meiotic products (Jang et al., 2018a).

Among the Cretan allotetraploids, Group I is cytologically the most diverse with several chromosome numbers ($2n = 4x = 25$-28), depending on the number of free chromosomes 6 and 7, and the number of fusion chromosomes F^1 (6-7), but stable number of chromosomal arms (figure 3). Loci of satellite DNA *PaB6* are present in pericentric regions of all chromosomes of this group, 5S rDNA is present in all four chromosomes 1 and 2, and 35S rDNA in all chromosomes 3. Genomic *in situ* hybridization (GISH) indicates homogenization of all chromosomes towards B^6B^6 maternal parent. The remaining three allotetraploid groups all

possess $2n = 4x = 28$ chromosomes, lacking the F^1 fusion chromosome and therefore can only be distinguished using mapping of the tandem repeats and genome size measurements. Group II genome consists of two chromosome sets nearly identical to those of Group I plants with $2n = 4x = 28$ chromosomes and two sets of the B^7B^7 type II chromosomes. This is consistent with the presence of fourteen *PaB6* signals, three 5S rDNA signals on chromosomes 1 (one single of B^6 origin and one duplicated of B^7 origin) and two on chromosome 2 of B^6 origin, as well as two 35S rDNA signals on chromosomes 3 of B^7origin (occasionally accompanied by a weaker third signal). Finally, Groups III and IV represent backcrosses of the Group II plants to either Group I allotetraploids with $2n = 4x = 28$ chromosomes or B^7B^7 diploids, respectively. Group III genome comprises 21 chromosomes of Group I and seven of Group II origin with 21 *PaB6* signals, five 5S rDNA signals on chromosome 1 (three single of Group I origin and one duplicated of Group II origin) and three 5S rDNA signals on chromosome 2 of Group I origin and four 35S rDNA signals on all chromosomes 3. In Group IV, 21 chromosomes are of B^7origin, as a result of the backcrossing with the diploid B^7B^7 cytotype, and seven are inherited from Group I $2n = 4x = 28$ plants. *PaB6* signals are therefore present on seven chromosomes, while five signals of 5S rDNA are found in chromosomes 1 (one single of Group II origin, one duplicated and two single of B^7origin) and one in chromosome 2 of Group II origin. 35S rDNA is located in all four chromosomes 3, three of them being of B^7origin and the remaining one of Group II origin. Mapping of satellite DNA *PaB6* alone is therefore sufficient for assigning allotetraploid individuals with $2n = 4x = 28$ chromosomes to the four Groups. This can be determined as follows: 28 *PaB6* signals correspond to Group I, 21 to Group III, 14 to Group II, and 7 to Group IV (Jang et al., 2018a).

Cytogenetic analyses prior to the identification of four allotetraploid Groups on Crete, indicated a geographical structure of the occurrence of plants possessing $2n = 4x = 26$ and $2n = 4x = 28$ chromosomes (Figure 5). Group I allopolyploids with $2n = 4x = 26$ chromosomes (plants with $2n = 4x = 25$ and 27 have been considered aberrant) have only been reported from the easternmost part of the island. In contrast, the $2n = 4x = 28$ plants, whose origin cannot be determined based solely on chromosome number, have been reported in localities surrounding the Dikti Mountains. Although there is a slight extension of this distribution toward the central region, it remains primarily centered in the east, and not extending either to the island's far eastern edge or to coastal areas. The hexaploid *Prospero elisae* Speta ($2n = 6x = 42$) has also been documented from the eastern part of Crete further illustrating the cytogenetic complexity of the group within this geographic system. Although *Prospero autumnale* is widespread in the

Balkan Peninsula, it cannot be reliably distinguished morphologically and thus its identification is based solely on its karyological profiles. Furthermore, it is worth mentioning that *Prospero talosii* (Tzanoud. & Kypr.) Speta, another member of the complex with the remarkable chromosome number of approximately $2n \approx 150$, has been described from the nearby islet of Dia (Tzanoudakis & Kypriotakis, 1998). This species is known from just two localities, with a few individuals reported. The presence of significantly broader leaves of this cytotype, reaching around 3cm in width, led to comparisons with *Prospero obtusifolium* (Poir.) Speta (Hamouche et al., 2010). However, lack of in-depth karyological analysis does not allow for more precise comparison of this cytotype to known diploids and tetraploids. Nevertheless, it represents another example of the karyological plasticity of the polyploids within the complex.

B chromosomes and supernumerary chromosomal segments

To complicate the chromosomal diversity even further, both supernumerary B chromosomes (chromosomes that do not recombine with the A-chromosome complement and so are exempted from strictly Mendelian inheritance, referred to as Bs) and supernumerary chromosomal segments (SCSs), have been found in all the diploid cytotypes and in many of the polyploids (Jang et al., 2016, 2018b). The great plasticity of the genome of *Prospero autumnale* has an impact on the persistence and recurrent origin of such elements, since they are hypothesized to be remnants of chromosomal rearrangements. The occurrence of Bs is quite challenging to be structured and categorized, given their complex origin pathways and evolutionary trajectories. All Bs in *Prospero autumnale* complex are highly variable in repeat content, morphology and size, with up to six Bs reported in one individual. Only one B chromosome variant (in AA cytotype) was inferred to have been established in this cytotype and be of older origin, with all other Bs hypothesized to be of a more recent and recurrent origin. An independent origin is also likely for the B chromosome in the B^6B^6 cytotype, as suggested by its lack of repetitive sequences (Jang et al., 2016).

Other genomic blocks that are present across the genus are the SCSs representing additional blocks of DNA permanently attached to some of the chromosomes of the complement. Their position in the genome of each cytotype is stable and each is likely of single origin, as these are shared among the diploid cytotypes. They are mostly terminal and increase the individual chromosome length up to 36.4%. In contrast to other plant groups with heterochromatic and interstitial SCSs, in *Prospero autumnale* complex those are euchromatic and terminal. Their numbers and significant polymorphic presence cannot be correlated with any phenotypic differentiation within cytotypes (Jang et al., 2018b). Their widespread presence in the complex

may have resulted from chromosomal rearrangements linked to the formation of new cytotypes with altered base chromosome numbers and karyotype structures. Some of these SCSs have been hypothesized to be quite old, with their origin likely predating the diversification of the existing diploid cytotypes. Chromosome 1 possesses SCS of similar size across the geographical range and ploidy levels of the complex, suggesting its common origin. This ancestral SCS has been hypothesized to be the result of an early translocation of a B chromosome during the diversification of the complex and it can be identified in all cytotypes using GISH with B^7 genomic DNA. In contrast, other SCSs may vary in age, with some potentially still being formed recurrently (Jang et al., 2018b).

Aim of the study

The combination of all unique characters of the highly dynamic genomes of *Prospero autumnale* complex, highlights the necessity of extensive phylogenomic, cytogenetic and morphological analyses of the group before drawing any conclusions about the relationships between cytotypes and their taxonomic status. Due to low levels of phenotypic differentiation among cytotypes and high levels of morphological character variation combined with high levels of structured chromosomal variation, analyses of karyotypes and genome sizes are crucial for assigning individuals to cytotypes (Jang et al., 2013, 2018a). Therefore, unlike in many other plant groups for which simpler approaches are sufficient, detailed cytogenetic analyses of each individual of *Prospero autumnale* complex are prerequisite for any other analyses. Only then further taxonomic, biogeographical, phylogenetic and evolutionary questions can be addressed. Phylogenetic analyses of selected nuclear (ITS1+2) and plastid regions supported the recognition of the cytotypes as distinct evolutionary lineages (Jang et al., 2018a). Initial large-scale morphological analyses of multiple individuals representing various cytotypes from different geographical regions within the species distribution range did not provide support for treatment of these cytotypes as separate taxonomic entities (Jang, 2013; Vestek et al., 2019). Although some morphological traits were identified as potentially diagnostic, the extensive variation and overlaps among cytotypes, especially with confounding effects of allopolyploidy, resulted in insufficient resolution (Jang et al., 2013, 2018a).

Quite some new species have been described within the complex over the years, mostly based on analyses of only a few individuals of a single population (Tzanoudakis & Kypriotakis 1998; Speta, 2000; Rukšāns, 2007; Brullo et al., 2009; Firat & Yildirim, 2016). Most of these species were described before the existence of structured chromosomal and genomic variation has been understood. This, therefore, raises questions about the taxonomic validity of the specific

segregates, especially considering that diploid and polyploid cytotypes may occur sympatrically. In all instances, the validly described species represent local segregates, as their presence has not been recorded beyond their type localities, as clearly is the case on the small area of the island of Crete. Six species have been validly described as endemics of Crete, each known only from a single locality and a single collection (Speta, 2000; Strid, 2016). Of these, four were identified as diploids: *Prospero depressum* Speta, *Prospero idaeum* Speta, *Prospero rhadamanthi* Speta, and *Prospero minimum* Speta, and two as tetraploids: *Prospero battagliae* Speta and *Prospero hierapytnense* Speta (Figure 5, Table 1). Despite some degree of morphological differentiation observed both *in situ* and *ex situ*, these taxa still possess largely similar and overlapping trait combinations, hindering clear taxonomic identification. This morphological complexity has so far precluded the development of a consistent and practical identification key.

This study, therefore, aims to test the taxonomic status of these six species of the island of Crete using an integrative approach with the emphasis on genomic identification of the cytotypes, implemented with detailed morphological analyses of multiple individuals of each population and basic phylogenetic analyses. To date, neither the cytotype "purity" of these populations nor the presence of similar morphotypes elsewhere has been investigated, as no further studies have been conducted since their initial taxonomic description. One of the important characters used for species description was the chromosome number. However, in the light of more recent genomic analyses, it is clear that chromosome number alone is not sufficient for cytotype identification (Jang et al., 2018a), especially for polyploids with $2n = 4x = 28$.

To this end, morphological, genomic, phylogenetic, and chromosomal analyses were performed on multiple individuals of the six abovementioned species (Table 1) collected from their six *loci classici* and subsequently cultivated in the Botanical Garden of the University of Vienna. These analyses aimed to test the specific status of the taxa and to better understand their evolutionary distinctiveness and the processes shaping this complex. The primary objective of this study was (1) to test the cytotype uniformity within the populations, (2) to compare the karyotypes with the already described chromosomal races, (3) to assess the extent of morphological differentiation within and among six species/populations, (4) to compare current character states with those documented in the original species description (5) to examine the phylogenetic relationships of selected individuals.

Specifically, morphological characters, both vegetative and reproductive, were analysed in 10 individuals from each of the six *loci classici* on Crete (Figure 5). Additionally, genome sizes were measured using flow cytometry and the chromosome numbers and karyotypes were established. The two polyploid species were also analysed using FISH with repetitive DNAs to determine their origin and type, considering the genomic diversity among allotetraploid cytotypes documented on the island (Jang et al., 2018a). Finally, phylogenetic analyses of the nuclear ITS1+2 regions of selected individuals were conducted within the existing larger phylogenetic framework (Jang et al., 2018a) to test whether the species/populations represent evolutionarily well-defined and distinct lineages. The combined results of all these approaches allowed the testing of the taxonomic status of these six *Prospero* Salisb. species. More broadly, the study also contributes new insights into the dynamic evolution of the plant species complex and provides additional data for future analyses of plant groups whose diversification may largely be driven by chromosomal change.

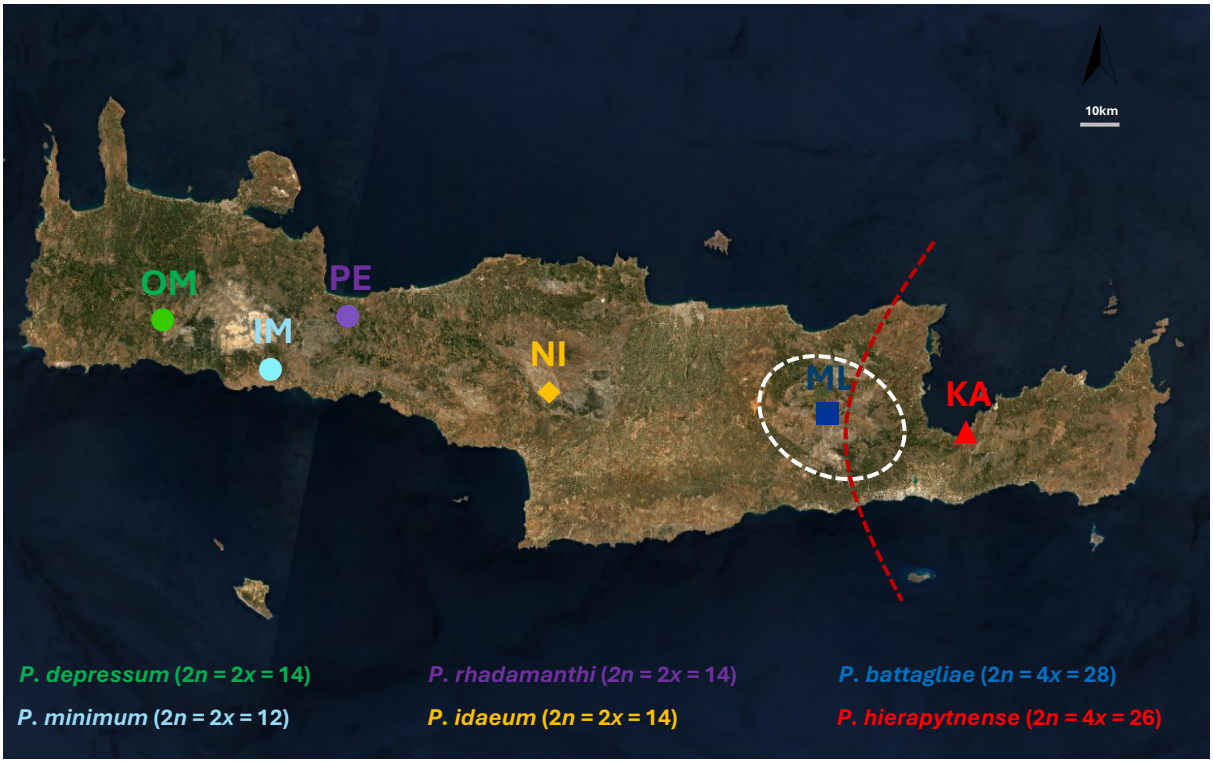

Figure 5. Map of the *loci classici* of the six endemic *Prospero* Salisb. species on Crete. OM: Omalos seasonal lake, IM: Imbros gorge, PE: Petre gorge, NI: Nida plateau, ML: Mesa Lasithi plateau, KA: Kavousi gorge. Dashed circle indicates the area in which $2n = 4x = 28$ have been reported. Individuals possessing $2n = 4x = 26$ have only been reported to the east of the red dashed line. Base map retrieved from Copernicus Sentinel-2 imagery 2021 processed by EOX.

Table 1. Morphological traits of the endemic *Prospero* Salisb. species on Crete as documented in their original description (Speta, 2000).

Species	Bulb	Root	Leaf	Scape	Pedicels	Perianth	Filament	Ovary	Style	Capsule	Seed
P. depressum ($2n = 2x = 14$)	White inside, 3.5-4 cm long, 1.7-2 cm in diameter. Coat brown.	Thick, branched	Leaves 10-15, green, up to 3-5 mm wide, 10 cm long, appearing in autumn.	Ascending, 4-8 cm long during flowering, 0.8-1.2 mm in diameter, with 5-18 flowers, up to 6-10 cm long at fruit maturity.	1.5-3 mm long during flowering, up to 3-5 (-7) mm at fruit maturity.	Whitish tepals, 5.5 mm long, 2 mm wide, with a green-brown midrib.	Lanceolate, pale pink, 3.6 mm long, 0.9 mm wide at base, white.	Ovoid, white, 2.4 mm long, 1.4 mm in diameter.	2 mm	3 mm	Black, 2.8 mm long, 1.5 mm wide.
P. minimum ($2n = 2x = 12$)	White inside, subglobose to ovoid, 1.1-1.8 cm long, 0.7-1.4 cm wide. Coat brown.	Few-branched	Filiform, 0.5-1 mm wide, 6-10 cm long, appearing in autumn.	Straight, slender, 1-2 (-3), 0.7-1.2 mm in diameter, 4-10 cm high during flowering, up to 17 cm at fruit maturity, with 3-10 flowers.	2-6 mm long during flowering, up to 2 cm at fruit maturity.	Rose-colored tepals, 4.8-5 mm long, 2 mm wide, with a rusty midrib.	Broadly lanceolate, violet, 3-3.5 mm long, 1 mm wide at base, white.	Subglobose, violet, 1.3 mm in diameter.	1-1.3 mm	2.5-3 mm	Dark brown-black, 1.5 mm long, 1 mm wide.
P. rhadamanthi ($2n = 2x = 14$)	Subglobose to ovoid, 1.6-2 cm long, 1.3-1.8 cm wide, whitish inside. Coat brown.	Branched	Leaves 5-14 (-20), green, up to 1.2-2 mm wide, up to 20 cm long, appearing in autumn.	Straight, 1 mm in diameter, 12-16 cm high during flowering, up to 18 cm at fruit maturity, with 5-28 flowers.	4-7 mm long during flowering, up to 2 cm at fruit maturity.	Pale pink tepals, 6 mm long, 2 mm wide, with a green midrib.	Lanceolate, pale pink, 4 mm long, 1 mm wide at base, white.	Pale violet, 2 mm long, 1.5 mm in diameter.	1.8 mm	3 mm	Black, 1.8-2 mm long, 1 mm wide.
P. idaeum ($2n = 2x = 14$)	Subglobose to broadly ovoid, whitish inside, 2-3 cm in diameter. Coat rusty-colored.	Branched	Leaves 7-14, up to 2-7 mm wide, 11-15 cm long, appearing in autumn.	Straight, 2-3, 1.2-1.4 mm in diameter, 10-18 cm high during flowering, 9-14 cm at fruit maturity, with 7-15 flowers.	4-5 mm long during flowering, up to 10-12 mm at fruit maturity.	Pale pink, lanceolate tepals, 3 mm long, 1 mm wide at base, white.	Lanceolate, pale pink, 3-4 mm long, 1 mm wide at base, white.	Ovoid, lilac, 1.6 mm long, 1.3 mm in diameter.	1.7 mm	3 mm	Black, 1.8 mm long, 1 mm wide.
P. battagliae ($2n = 4x = 28$)	Globose to ovoid, 1.1-2.8 cm in diameter, pink inside. Coat rusty-colored.	Branched	Leaves (4-) 8-15 (-19), green with wine-colored base, up to 1.5-2 mm wide, 18-20 cm long, appearing in autumn.	Straight, 1-3, 11-20 cm long, 1.2 mm in diameter, up to 20-25 cm high at fruit maturity, with 6-20 flowers.	4-8 mm long during flowering, up to 3 cm at fruit maturity.	Pale violet tepals, 6-7.5 mm long, 2-2.6 mm wide, with a green midrib.	Linear, short-acuminate, violet, 5 mm long, 1 mm wide at base, white.	Ovoid violet, 2-2.5 mm long, 1.5 mm in diameter.	2-2.5 mm	4mm	Black, 2-2.5 mm long, 1 mm wide.
P. hierapytnense ($2n = 4x = 26$)	Ovoid, 1.5-2 cm long, 0.9-2 cm wide, pale pink or white inside. Coat brownish.	Branched	Leaves 6-9, 1-2 mm wide, 10-12 cm long, appearing in autumn.	Straight, 1-2, 7-15 cm long, 1.2-1.5 mm in diameter, with 6-14 flowers.	5-8 mm long during flowering, up to 2 cm at fruit maturity.	Pink tepals, 5.5-6.5 mm long, 2-2.5 mm wide.	Lanceolate, pink, 3-4 mm long, 1-1.2 mm wide at base, white.	Violet ovoid, 2 mm long, 1.6 mm in diameter.	1.5-1.8 mm	3 mm	Black, 1.6 mm long, 1.2 mm wide.

Materials and Methods

Plant material

Plants from the six *loci classici* of the local endemics *Prospero* Salisb. species in Crete were collected during September–October 2024. For each species, 20–30 individuals were sampled, except for locality KA, for which only 10 individuals were found at the time of collection. For each plant, the scape was removed and dried in an herbarium press for morphological analysis, while the corresponding bulb was planted in the Botanical Garden of the University of Vienna. The cultivated plants were used for cytological analysis, and for the further morphological analyses of the vegetative organs, matching field-collected inflorescences. The type localities corresponded to the original species descriptions. Material was labelled using the abbreviation of each locality (Figure 5) and numbered consecutively.

Omalos seasonal lake (OM)

The Omalos plateau (Chania province) is located in the western part of Crete and is part of the Lefka Ori mountains. A seasonal lake lies at its southern edge, from where *Prospero depressum* Speta was first described. Specimens were collected from the upper limit of the coastal section. This locality is referred to as (OM) in this study and is situated at 1063m elevation, at coordinates 35°19'27.60"N, 23°53'27.91"E.

Imbros gorge (IM)

Imbros gorge (Chania province) was originally reported as the type locality of *Prospero minimum* Speta at an altitude of 550 m. However, during a visit to this exact site, it appeared unlikely for the species to grow there due to the narrowness of the gorge at that point, which facilitates continuous water flow. Individuals were instead found approximately 100m higher, where the gorge widens, in open area along the main path. The population appears to extend between 750–850m, with additional occurrences reported (M. Choreftakis, pers. comm.). This locality is referred to as (IM) in this study, with the exact collection point situated at 660m elevation, at coordinates 35°14'21.48"N, 24°09'56.40"E.

Petre gorge (PE)

The *locus classicus* of *Prospero rhadamanthi* Speta is the small Petre gorge in Rethimno province. During an initial visit in late September, no individuals were found. A week later, a

single, locally confined population was discovered in the upper part of the gorge. By the end of October 2024, additional plants were reported near the gorge entrance, approximately 5 m in elevation (M. Choreftakis, pers. comm.), but were not sampled for this study, as the collected material originated from the originally designated site. This locality is referred to as (PE) in this study, with the exact collection point situated at 49 m elevation, at coordinates 35°19'27.90"N, 24°21'43.47"E.

Nida plateau (NI)

Mount Psiloritis hosts the Nida plateau (Rethimno province), the highest in Crete, covering approximately 1.5 km². Several smaller upland basins are also found nearby. The area is used as grazing land but remains unused for cultivation due to its high elevation. Despite extensive surveys across the plateau, *Prospero idaeum* Speta was observed only in a single, limited patch, consistent with its originally reported distribution. This locality is referred to as (NI) in this study, with the exact collection point situated 1351m elevation, at coordinates 35°12'4.92"N, 24°50'17.97"E.

Mesa Lasithi plateau (ML)

The broadest locality, based on the original species description of the polyploid *Prospero battagliae* Speta, is the Mesa Lasithi plateau (Lasithi province). A large population was observed along a stream at the easternmost edge of the plateau, near the entrance to a small gorge. The area is heavily used for agriculture, and although the species may have once had a wider distribution there, it now likely persists only in isolated, undisturbed patches. This locality is referred to as (ML) in this study, with the exact collection point situated at 874m elevation, at coordinates 35° 9'55.41"N, 25°31'22.80"E.

Kavousi gorge (KA)

In eastern Crete, Kavousi gorge (Lasithi province) marks the *locus classicus* of *Prospero hierapytnense* Speta, with its originally described distribution of less than 1 km^2. A small population of only 10 individuals was observed at the upper limit of the locality. Upon searching the soil more broadly, based on the assumption that additional individuals might be present, several bulbs were collected and later used for cytological analysis. This locality is referred to as (KA) in this study, with the exact collection point situated at 220m elevation, at coordinates 35° 7'8.03"N, 25°52'10.18"E.

Morphological analysis

A total of 19 quantitative morphological characters were measured under a stereomicroscope using the dried herbarium specimens. Due to the hysteranthous nature of the genus, leaf dimensions were obtained after the first seasonal *ex situ* growth, which occurred 2–4 months post-transplantation, depending on the population. Measurements were taken from 10 individuals per species/population, limited by the availability of *Prospero hierapytnense* Speta individuals. These data were then used in multivariate morphometric analyses and compared with measurements from the original species descriptions to assess morphological consistency over time. Qualitative characters were also documented but not used in any analysis.

Morphometrics

Morphometric analyses were conducted using the R package MorphoTools2 (Šlenker et al., 2022). Multiple Principal Component Analyses (PCA) based on a correlation matrix, were performed using different combinations of the measured characters. The first two principal components were visualized to assess interspecific variation. These analyses were performed either including or excluding bulb size to evaluate its significance. Analyses were also performed using different cytotype combinations to determine whether the general discrimination pattern was influenced by cytotype.

Comparison with original descriptions

To assess the stability of morphological features and population uniformity over time and the validity of the species descriptions, comparative boxplots were generated using the ggplot2 R package (Wickham, 2016). These plots were based on trait data from the original species descriptions (Speta, 2000), alongside the observed ranges of these traits from the current study. This analysis was conducted independently for each morphological character, and the variation observed was visualized to compare the two datasets.

Karyotype analysis

Feulgen staining, chromosome preparation and karyotype assembly

Bulbs were carefully removed from soil and briefly rinsed with tap water to eliminate excess dirt. Healthy actively growing root-tip meristems were selected, transferred to small bottles, and pretreated with 0.05% aqueous solution of colchicine (Sigma, Vienna, Austria) for four hours at room temperature in darkness. The solution was then removed, the material was briefly

washed with tap water and immediately fixed in freshly prepared ethanol: acetic acid (3:1) and stored at -20°C until use.

Chromosome numbers were established using standard Feulgen staining and squash technique. The fixed root-tip meristems were transferred to tubes containing 5N HCl (VWR, Vienna, Austria). After 20 minutes of incubation, HCl was carefully removed and material was washed with tap water. Subsequently, the Schiff's reagent (Sigma, Vienna, Austria) was added to the material and incubated at room temperature in darkness for 60 minutes. The root-tip meristems were then transferred onto a pre-cleaned slide into a drop of 60% acetic acid (VWR, Vienna, Austria). Any other tissue (e.g. root cap and xylem) was carefully removed using entomological needles and the meristems were dissected under the stereomicroscope. A coverslip was placed and gently squashed using the tip of the needle, and further pressure was applied using the thumb. The samples were analysed under the light microscope Axioplan (Carl Zeiss, Vienna, Austria) and chromosomal spreads were photographed with CCD monochrome camera and Axiovision software (Carl Zeiss, Vienna, Austria).

Mitotic metaphase chromosomes from well-spread plates were cut out using the CorelPhoto Paint software. For each analysed individual at least one karyotype was cut-out with chromosomes paired and pairs arranged in decreasing order of chromosome length. The only exceptions were the B^6B^6 and Group I allopolyploids plants for which the large sub-metacentric fusion chromosome (F^1 (6-7); Jang et al., 2013), was placed as last, in allotetraploids of Group I together with its homoeologous free chromosomes 6 and 7 (Jang et al., 2018a).

Genome size estimation by flow cytometry (FCM)

The 1C values (pg) of all six species/populations were measured using flow cytometry using internal standard. Two plant species were used as standards, *Pisum sativum* (4.42 pg/1C (Greilhuber & Ebert, 1994)) and *Solanum pseudocapsicum* (1.29 pg/C (Temsch et al., 2010)) for each examined sample, due to the known genome size range of *Prospero autumnale* diploid and derived polyploid cytotypes (Jang et al., 2013, 2018a), making sure that the G1 peak of the standard did not overlap with the G1 peak of the sample. Fresh leaf material of a standard was initially chopped separately for the first calibration run. Subsequently, one fresh leaf per sample was co-chopped with one of the two standards in the same Petri dish using 1.1mL (550µL for chopping and 550µL for washing off) of the Otto's isolation buffer I (pH 1.5; Otto et al., 1981). The liquid fraction was filtered through a 30 mm nylon mesh (Saatilene Hitech, Sericol, Germany) to labelled tubes, and an additional 50mL of RNase A (0.15 mg RNase A per mL

suspension of nuclei) was added to each tube. Tubes were gently stirred and incubated in water bath at 37°C for 30 minutes to remove the RNAs. Finally, the nuclei were stained with 2ml of the light-sensitive staining Otto´s II buffer (pH 9.5; Otto et al., 1981) containing propidium iodide (PI; Sigma, Vienna, Austria) for a minimum of one hour in the refrigerator (4°C). The samples were measured using CyFlow ML flow cytometer, equipped with green laser (2x Cobolt Samba 532nm,100mW and 1x MSL532-30 532nm, 30mW). Three runs per sample were conducted by measuring 3333 particles per run with the exception of the individuals OM6, OM22, NI11, NI12 for which only two measurements were performed due to scarcity of the material. A value was accepted if the Coefficient of Variation (CV) of G_0/G_1 peaks was below or around 5%. To calculate the 1C-value of the samples, the ratio of sample/standard G1-peaks was multiplied by the 1C-value of the used standard (pg). In the case where both standards were appropriate for a specimen, the final mean value with lower coefficient of variation (CV) was used.

Fluorescence *in situ* hybridization (FISH)

The fixed root meristems were washed twice for 10–15 minutes in citrate buffer (pH 4.8; Jang & Weiss-Schneeweiss, 2015) and incubated in a pre-warmed enzyme mixture containing 0.4% pectolyase, 0.4% cytohelicase, and 1% cellulase in citrate buffer (pH 4.8) for 30 minutes at 37 °C. Following enzymatic digestion, the material was briefly washed in citrate buffer and transferred to 45% acetic acid. Dissection of the meristematic cells was carried out under a stereomicroscope, cover slips were applied and the cells were squashed. Quality of chromosomal spreads was checked using phase-contrast microscopy (Carol Zeiss, Vienna, Austria), and cover slips were removed after freezing the slides at -80°C. Slides were subsequently air dried and stored at 4°C until use.

Two satellite DNA monomers identified in *Prospero autumnale* were used as probes: *PaB6* (249 bp; Emadzade et al., 2014) and *Pa138* (Weiss-Schneeweiss, unpubl.). Both probes were commercially synthesized and labelled with either digoxygenin or biotin (Sigma Aldrich, Vienna, Austria). The fluorescence *in situ* hybridization procedure followed the protocol of Jang and Weiss-Schneeweiss (2015) and included the following steps: chromosome refixation, pepsin treatment to remove the cytoplasmic proteins, denaturation of chromosomal DNA and the probes, hybridization, stringent washes, detection of the labels using antibodies, staining of the chromosomal DNA with DAPI (Sigma, Vienna, Austria) and mounting the slides in antifade buffer. Probe *Pa138* was labelled with biotin and detected using ExtrAvidin-Cy3 (Sigma, Vienna, Austria) and probe *PaB6* was labelled with digoxigenin and detected with anti-DIG

antibody conjugated with FITC (Sigma, Vienna, Austria). Preparations were examined using an AxioImager M2 epifluorescence microscope (Carl Zeiss, Vienna, Austria), and images were captured with a CCD camera and ZEN software (Carl Zeiss, Vienna, Austria). Image processing was performed using Adobe Photoshop and Inkscape software using only the functions that applied equally to the whole image.

Phylogenetic analysis

DNA extraction

Total genomic DNA was extracted using the DNeasy Plant Mini Kit (QIAGEN, Hilden, Germany). A total of 18 individuals were used, three from each locality. 3–26 mg of dried silica-dried leaf tissue was used per individual, depending on the available material. DNA concentration was measured using a NanoDrop® ND-1000 spectrophotometer (Thermo Fisher Scientific, Vienna, Austria) and DNA quality was assessed by 1% (w/v) agarose gel electrophoresis. All the samples were then treated with RNase A for 30 minutes in 37°C and stored at -20°C until use.

PCR amplification and cycle sequencing

Primers anchored in 18S and 25S rDNA designed to amplify internal transcribed spacers 1 and 2 (ITS1+2) of 35S rDNA monomers (Jang et al., 2018a) were used for polymerase chain reactions (PCR). The amplified region included ITS1, the 5.8S rRNA gene, and ITS2. PCR reaction contained 0.25 μM of each primer, 1X DreamTaq PCR Master Mix (Thermo Fisher Scientific, Vienna, Austria) and genomic DNA diluted 1:50. Reactions were performed on an ABI 9700 thermal cycler (Applied Biosystems, Foster City, CA, USA) using the following conditions: an initial hold at 96°C for 3 minutes, followed by 35 cycles of 98°C for 30 seconds, 62°C for 30 seconds, and 72°C for 1 minute, with a final elongation at 72°C for 8 minutes. PCR products were analysed on a 1% (w/v) agarose gel.

Purification of the PCR products was carried out using Exonuclease I (Thermo Fisher Scientific, Vienna, Austria) and Thermosensitive Alkaline Phosphatase, (Thermo Fisher Scientific, Vienna, Austria) according to the manufacturer's protocol. Standard cycle sequencing was performed using the same primers as those for the amplification but at the concentration of 4 pmol and the BigDye Terminator v3.1 Cycle Sequencing Kit Mix (Thermo Fisher Scientific, Vienna Austria). For each PCR product two cycle sequencing reactions were

set up (one for the forward and one for the reverse primer). The cycling conditions were as follows: initial denaturation at 96°C for 1 minute followed by 35 cycles of 96°C for 10 seconds, 50°C for 3 minutes, and 60°C for 3 minutes. Sanger sequencing was conducted on an ABI 3730 DNA Analyzer (Thermo Fisher Scientific, Vienna, Austria).

Phylogenetic inferences

The ITS1-5.8S-ITS2 DNA sequences were assembled using SeqMan II (Lasergene, Madison, WI, USA) and manually aligned in BioEdit version 7.0.5.3. These sequences were then aligned to a larger dataset of 40 previously analysed *Prospero autumnale* individuals (Jang et al., 2013, 2018a). This larger dataset included *Prospero obtusifolium* (Poir.) Speta, *Prospero hanburyi* (Baker) Speta, and multiple cytotypes of *Prospero autumnale*, including diploid AA, B^7B^7, and B^6B^6 individuals and tetraploid AAB^7B^7, $B^7B^7B^7B^7$, and $B^6B^6B^7B^7$ individuals. The latter group of Cretan allotetraploids included individuals of all four genomic groups (Groups I-IV; Jang et al., 2018a). Additionally, one individual of *Othocallis siberica* (Andrews) Speta (subfamily Scilloideae) was used as the outgroup. The combined dataset was analysed using Maximum Likelihood (ML) with 1,000 bootstrap replicates in MEGA12 (Kumar et al., 2023) using the Tamura-Nei substitution model (Tamura & Nei, 1993). The final alignment was 656 bp long and encompassed 58 sequences. Branches with bootstrap support lower than 80 were collapsed. The consensus tree was edited using Inkscape and Microsoft PowerPoint.

Table 2. Plant material studied, including locality, chromosome number (2*n*), genome size (pg/1C±SD), number of *PaB6* signals, availability of ITS and morphometric data (Morph.), and corresponding figures.

Individual	Locality	2*n*	pg/1C (±SD)	*PaB6*	ITS	Morph.	Figures
OM3	Omalos seasonal lake	14	-	-	-	✓	11A
OM6	Omalos seasonal lake	14	4.58±0.06	-	✓	✓	8A,11A,14
OM7	Omalos seasonal lake	14	4.46±0.03	-	✓	✓	8A,11A,14
OM9	Omalos seasonal lake	-	-	-	-	✓	11A
OM10	Omalos seasonal lake	-	4.58±0.06	-	✓	✓	7A, 8A,11A,14
OM11	Omalos seasonal lake	14	-	-	-	✓	11A
OM12	Omalos seasonal lake	14	-	-	-	✓	11A
OM13	Omalos seasonal lake	14	-	-	-	✓	6A,11A
OM14	Omalos seasonal lake	14	-	-	-	✓	10A,11A,14
OM15	Omalos seasonal lake	-	-	-	-	✓	11A
OM16	Omalos seasonal lake	-	4.73±0.09	-	-	✓	8A,11A
OM18	Omalos seasonal lake	-	-	-	-	✓	11A
OM22	Omalos seasonal lake	-	4.61±0.03	-	-	-	8A
IM1	Imbros gorge	12	6.38±0.02	-	-	✓	6B,11A
IM3	Imbros gorge	-	6.11±0.02	-	-	✓	8A,11A
IM5	Imbros gorge	12	-	-	✓	✓	11A,14
IM7	Imbros gorge	-	-	-	-	✓	10B,11A
IM8	Imbros gorge	12	6.11±0.03	-	-	-	8A
IM9	Imbros gorge	-	-	-	-	✓	11A
IM10	Imbros gorge	-	-	-	✓	✓	11A,14
IM11	Imbros gorge	-	-	-	✓	✓	11A,14
IM12	Imbros gorge	-	-	-	-	✓	11A
IM13	Imbros gorge	-	-	-	-	✓	11A
IM15	Imbros gorge	12+1B	6.47±0.07	-	-	-	6C, 8A
IM16	Imbros gorge	12	6.17±0.05	-	-	-	7B,8A
IM17	Imbros gorge	-	6.04±0.02	-	-	-	8A
IM18	Imbros gorge	-	6.02±0.01	-	-	✓	8A,11A
PE1	Petre gorge	12	-	-	-	✓	11A
PE2	Petre gorge	-	-	-	-	✓	11A
PE4	Petre gorge	-	-	-	-	✓	11A
PE5	Petre gorge	12	-	-	-	✓	10C,11A
PE6	Petre gorge	-	-	-	-	✓	11A
PE7	Petre gorge	-	-	-	-	✓	11A
PE8	Petre gorge	12	6.27±0.02	-	-	✓	7C,8A,11A
PE9	Petre gorge	12	6.21±0.02	-	✓	✓	8A,11A,14
PE10	Petre gorge	-	6.58±0.03	-	-	✓	8A,11A
PE11	Petre gorge	-	-	-	-	✓	11A
PE12	Petre gorge	-	6.23±0.03	-	-	-	8A
PE13	Petre gorge	12	6.19±0.01	-	-	-	8A
PE14	Petre gorge	-	-	-	✓	-	14
PE15	Petre gorge	12	6.33±0.02	-	-	-	8A
PE16	Petre gorge	12	6.21±0.03	-	-	-	6D,8A
PE17	Petre gorge	-	-	-	✓	-	14
PE23	Petre gorge	12	-	-	-	-	-
NI1	Nida plateau	-	4.30±0.01	-	-	✓	8A,11A
NI2	Nida plateau	-	-	-	-	✓	11A
NI3	Nida plateau	-	-	-	-	✓	11A
NI5	Nida plateau	-	-	-	✓	✓	6E,11A,14

Table 2. (continued) Plant material studied, including locality, chromosome number (2*n*), genome size (pg/1C±SD), number of *PaB6* signals, availability of ITS and morphometric data (Morph.), and corresponding figures.

Individual	Locality	2*n*	pg/1C (±SD)	*PaB6*	ITS	Morph.	Figures
NI6	Nida plateau	-	-	-	-	✓	11A
NI7	Nida plateau	14	4.32±0.03	-	✓	✓	8A,11A,14
NI8	Nida plateau	-	-	-	-	✓	11A
NI9	Nida plateau	-	4.39±0.02	-	-	✓	8A,11A
NI10	Nida plateau	-	-	-	-	✓	11A
NI11	Nida plateau	-	4.38±0.01	-	-	✓	8A,11A
NI12	Nida plateau	-	4.36±0.05	-	✓	-	8A,14
NI13	Nida plateau	14	-	-	-	-	-
NI15	Nida plateau	14	4.46±0.01	-	-	-	8A,10D
NI16	Nida plateau	14	-	-	-	-	-
NI18	Nida plateau	14	-	-	-	-	-
NI20	Nida plateau	-	4.39±0.01	-	-	-	8A
NI22	Nida plateau	14	4.31±0.02	-	-	-	8A
NI23	Nida plateau	-	4.39±0.01	-	-	-	7D,8A
NI24	Nida plateau	-	4.37±0.03	-	-	-	8A
ML1	Mesa Lasithi plateau	28	-	-	-	✓	11A
ML2	Mesa Lasithi plateau	-	-	-	-	✓	10,11A
ML3	Mesa Lasithi plateau	28	10.37±0.01	-	-	✓	8A,11A
ML4	Mesa Lasithi plateau	-	-	-	✓	✓	11A,14
ML5	Mesa Lasithi plateau	28	10.03±0.08	-	-	✓	8A
ML6	Mesa Lasithi plateau	-	-	-	✓	✓	11A,14
ML7	Mesa Lasithi plateau	-	-	14	-	✓	11A
ML8	Mesa Lasithi plateau	-	-	-	-	✓	11A
ML9	Mesa Lasithi plateau	-	10.19±0.02	-	-	✓	8A,11A
ML12	Mesa Lasithi plateau	-	-	-	-	✓	11A
ML13	Mesa Lasithi plateau	28	10.02±0.02	14	-	-	8A
ML15	Mesa Lasithi plateau	28	-	14	-	-	-
ML16	Mesa Lasithi plateau	-	10.80±0.03	-	✓	-	7E,8A,14
KA1	Kavousi gorge	27	-	-	-	✓	6G,11A
KA2	Kavousi gorge	-	12.50±0.08	-	✓	✓	8A,11A,14
KA3	Kavousi gorge	-	-	-	-	✓	11A
KA4	Kavousi gorge	-	12.17±0.02	-	-	✓	7F,8A,11A
KA5	Kavousi gorge	26	11.99±0.01	26	-	-	6H, 8A
KA6	Kavousi gorge	-	-	-	-	✓	11A
KA7	Kavousi gorge	26	11.87±0.08	-	✓	✓	8A,11A,14
KA8	Kavousi gorge	-	-	-	-	✓	10,11A
KA13	Kavousi gorge	-	-	-	-	✓	11A
KA17	Kavousi gorge	-	12.12±0.10	-	-	-	8A
KA18	Kavousi gorge	-	-	-	✓	✓	11A,14
KA19	Kavousi gorge	-	12.13±0.08	-	-	-	8A
KA21	Kavousi gorge	25	11.77±0.08	-	-	-	6I, 8A
KA24	Kavousi gorge	-	12.43±0.06	-	-	-	8A
KA25	Kavousi gorge	-	-	-	-	✓	11A

Results

Chromosome numbers and karyotype analysis

Fixed roots of a total of 31 individuals were analysed karyologically using Feulgen staining to establish the chromosome numbers, whereas the karyotypes were created for at least one individual per locality. The construction of karyotypes was guided by the convention described of Jang et al. (2013) for the diploids and Jang et al. (2018a) for the tetraploids. Specifically, NOR-bearing chromosome was always identified as chromosome 3, although in some cases it was smaller than chromosome 4, the large sub-metacentric fusion chromosome F^1(6-7) was always placed as last in the karyotype and the homologous and homoeologous chromosomes of the tetraploid individuals were always arranged in groups of four, rather than in pairs.

All the examined plants from OM and NI locality ($2n = 2x = 14$) possessed seven pairs of chromosomes (Figures 6A, E). Their karyotypes consisted of five sub-metacentrics (chromosomes 1, 2, 3, 5, 6), one sub-telocentric (chromosome 4) and one near-metacentric (chromosome 7). A NOR of chromosome 3 was adjacent to the centromere and located within the long arm. Six pairs of chromosomes were consistently present in populations IM and PE ($2n = 2x = 12$; Figures 6B, C, D). Individual IM15 possessed also a supernumerary small B chromosome ($2n = 2x = 12+1B$; Figure 6C). Each of the analysed IM and PE karyotypes consisted of four sub-metacentrics (chromosomes 1, 2, 3, 5), one sub-telocentric (chromosome 4) and one large sub-metacentric (chromosome 6), while the NOR was located interstitially within the long arm of both chromosomes 3. The four analysed tetraploids from ML locality all possessed 28 chromosomes ($2n = 4x = 28$; Figure 6F). Two of the four chromosomes of each type were larger besides chromosome 3 for which all four chromosomes were of similar size. Tetraploids of KA locality exhibited chromosome number variation with three different chromosome numbers found: $2n = 4x = 25$, 26 or 27 (Figures 6G, H, I). Specifically, individuals KA5 and KA7 possessed 26 chromosomes, while KA1 had 27, and KA21 had 25 chromosomes. The one, two or three large sub-metacentric F^1(6-7) fusion chromosomes were always grouped together with their homoeologous free chromosomes 6 and 7. In this tetraploid population, all four homologous/homoeologous chromosomes of each type were of similar size except for those chromosomes that carried terminal supernumerary segments in individuals KA1, on chromosome 1, and KA21, on one of the three F^1(6-7) fusion chromosomes (Figures 6G, I).

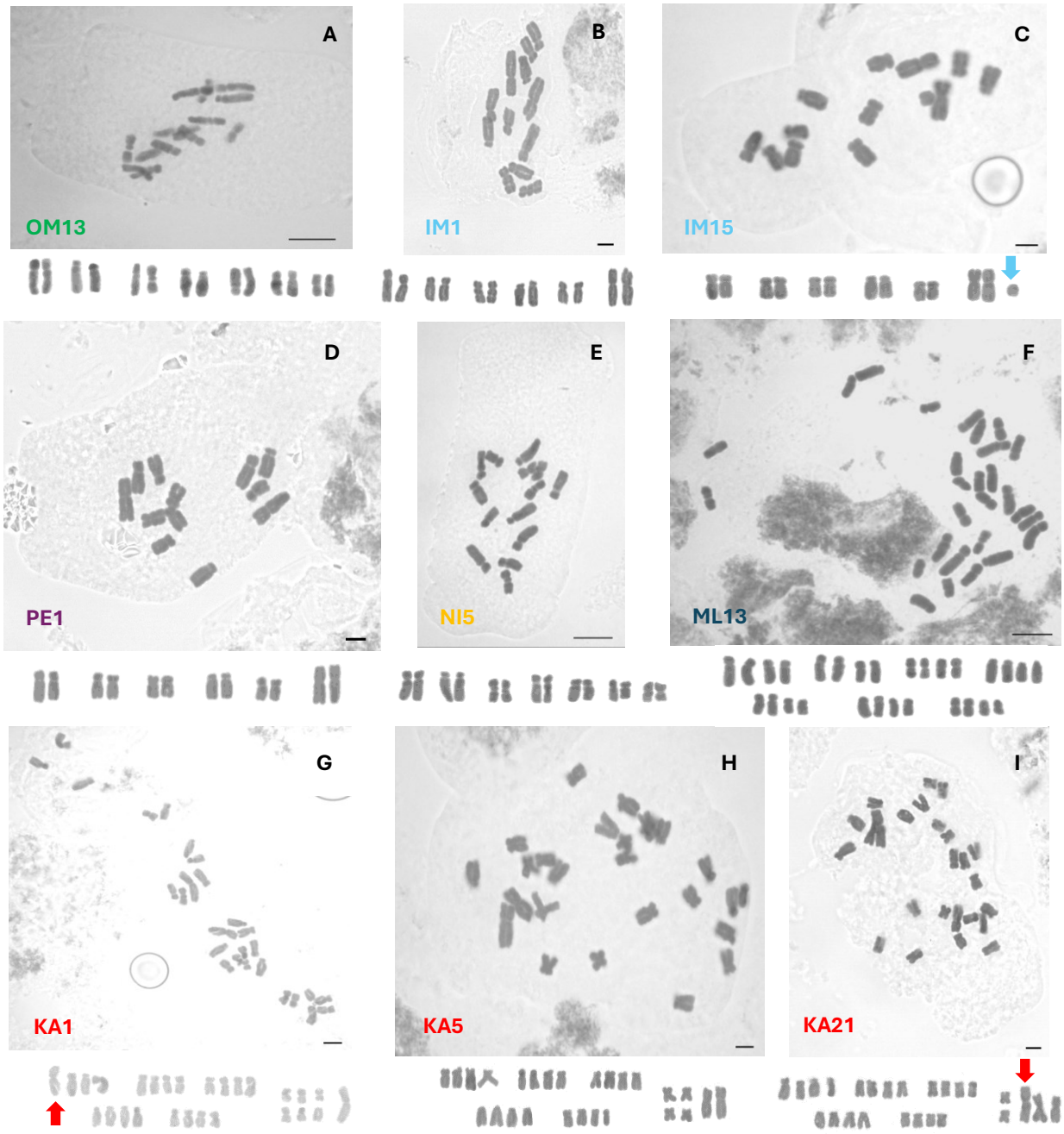

Figure 6. Mitotic metaphase chromosomes and karyotypes of analysed *Prospero* Salisb. individuals. A) Individual OM13 ($2n = 2x = 14$; B^7B^7); B) Individual IM1 ($2n = 2x = 12$; B^6B^6); C) Individual IM15 ($2n = 2x = 12 + 1B$; B^6B^6); D) Individual PE16 ($2n = 2x = 12$; B^6B^6); E) Individual NI5 ($2n = 2x = 14$; B^7B^7); F) Individual ML13: $2n = 4x = 28$; $B^6B^6B^7B^7$, Group II); G) Individual KA1 ($2n = 4x = 27$; $B^6B^6B^7B^7$, Group I); H) Individual KA5 ($2n = 4x = 26$; $B^6B^6B^7B^7$, Group I); I) Individual KA21 ($2n = 4x = 25$; $B^6B^6B^7B^7$, Group I). Light blue arrow indicates the B chromosome; red arrows indicate the supernumerary chromosomal segments (SCSs). Scale bar = 5 µm.

Genome size estimation by flow cytometry (FCM)

The genome size was measured for 42 individuals using the young leaves of the plants growing *ex situ*. At least five individuals were measured from each of the six localities. Two internal standards (*Pisum sativum* and *Solanum pseudocapsicum*) were used to ensure a proper interpretation of the results. The final 1C values were calculated as the average of three measurements performed for each sample with only a few exceptions (See Materials and Methods).

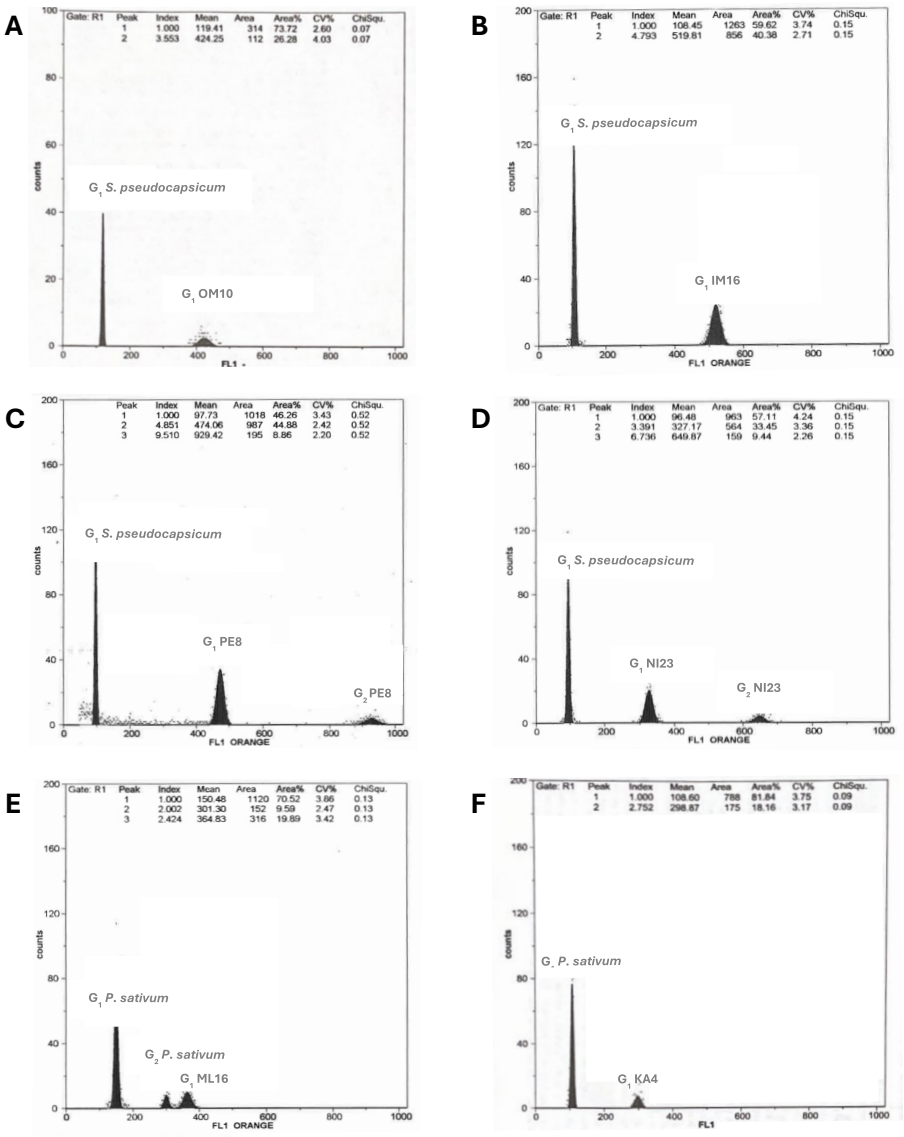

Figure 7. Flow cytometry histograms for one individual per locality: A) Individual OM10; B) Individual IM16; C) Individual PE8; D) Individual NI23; E) Individual ML16; F) Individual KA4. The CV values for each peak are indicated in the upper part of each graph.

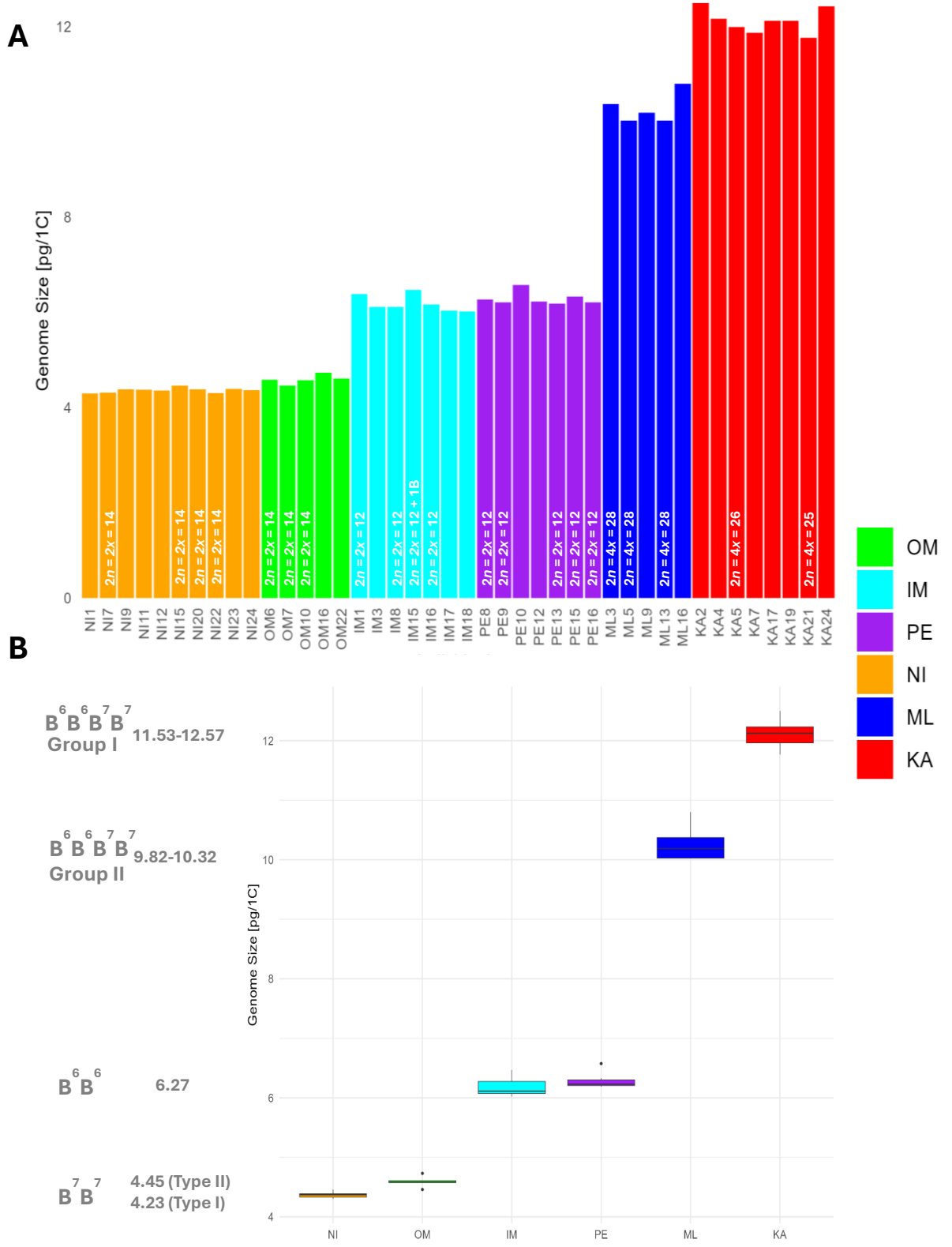

Figure 8. Genome sizes of analysed individuals. A) Genome sizes of all individuals grouped by locality. Individuals for which chromosome numbers have been established are indicated within individual bars; B) Comparison of genome size variation within individual localities with the reference genome sizes of each cytotype published previously (left side of the plot; Jang et al., 2013, 2018a).

The genome size for plants of the OM locality ($2n = 2x = 14$) fell in the range of 4.46-4.73 pg/1C. Leaf material in this group was more mucilaginous and these samples also exhibited the highest coefficient of variation (CV) values compared to individuals from other localities. The NI population ($2n = 2x = 14$) showed slightly lower, but comparable, genome sizes ranging from 4.30 to 4.46 pg/1C in 10 individuals, the highest number of samples analysed from a single locality. In contrast, plants from IM and PE localities (both $2n = 2x = 12$) exhibited higher genome size values, with ranges of 6.11–6.47 pg/1C and 6.19–6.58 pg/1C, respectively. The two allotetraploid populations, ML ($2n = 4x = 28$) and KA ($2n = 4x = 25$, 26 or 27) had the largest genomes as well as the highest levels of variation. These two populations also differed significantly from each other, with non-overlapping genome size ranges of 10.02–10.80 pg/1C for ML, and 11.77–12.50 pg/1C for KA (Figure 8). The values obtained for each examined population fell well within the known range for the previously described cytotypes (Figure 8B).

Fluorescence *in situ* hybridization (FISH)

Fluorescence *in situ* hybridization (FISH) was used to map two satellite DNAs identified previously in *Prospero autumnale*. The satellite repeat *PaB6* was used as the primary marker because the number of chromosomes carrying this pericentromeric satellite DNA allows for unambiguous identification of all four $B^6B^6B^7B^7$ allotetraploid groups. The satellite DNA *Pa138*, specific for B^6-genome has been included in an attempt to gain insight into its abundance in allotetraploid genomes. Analyses were conducted on one individual from the KA locality and three individuals from the ML locality, due to the uniformity of genome sizes of all individuals in these populations that is indicative of intrapopulational cytotype uniformity. In the KA5 individual, 26 *PaB6* signals were observed, corresponding to the total number of chromosomes (Figure 9A). In contrast, all individuals from ML exhibited 14 *PaB6* signals

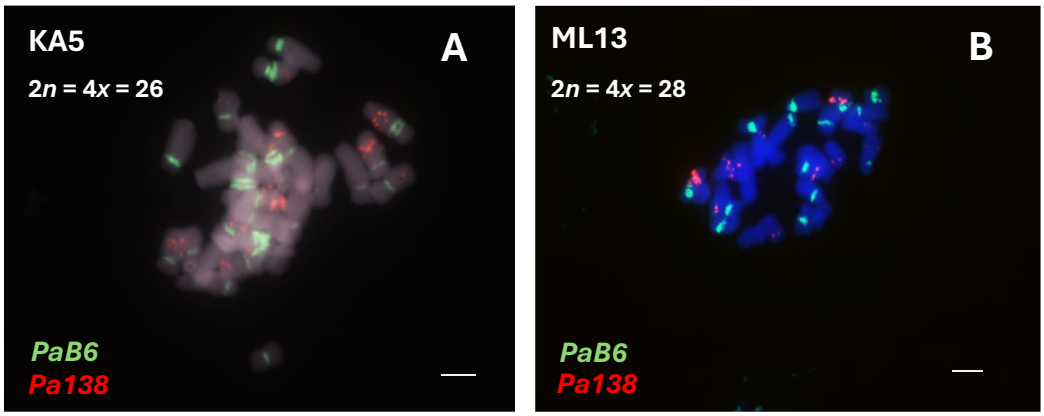

Figure 9. Localization of satellite DNAs *PaB6* and *Pa138* in mitotic metaphase chromosomes of the two polyploid individuals. A) Individual KA5 ($2n = 4x = 26$); B) Individual ML13 ($2n = 4x = 28$). Scale bar = 5 µm.

(Figure 9B, Table 2). Both individuals exhibited varying numbers (8-12) of smaller interstitial loci of satellite DNA *Pa138* (Figure 9).

Morphometric analysis

In total, 19 quantitative traits (Figure 11B) of 10 individuals per species/population were scored and analysed using principal component analysis (PCA). Various subsets were tested, e.g., excluding bulb sizes, or examining relationships between and within cytotypes. Grouping of the individuals of the populations, but not clear discrimination of the species, was consistently observed across all analysed combinations. PC1 never exceeded 36.33% of the explained variance (Figure 12E), and PC2 reached a maximum of 21.78% (Figure 12F), indicating modest but sufficient support for underlying structure in the data.

The inclusion of all six populations revealed significant overlap among them except for OM population, which appeared more distinct (Figure 11A). However, the exclusion of the bulb size resulted in less structured delimitation of this population with the lowest value of PC1 of all the analyses (Figure 12A). In both datasets, with and without the bulb characters, individuals from each locality generally clustered together, indicating certain levels of within-population uniformity, except for a few outliers, particularly from KA locality. Most of the vegetative characters together with the Number of Inflorescences (NoI), contributed strongly to the PC1 (Figure 11C). In contrast, floral traits together with Leaf Length (LL), contributed less significantly influencing both PC2 and, to a lesser extent, PC1 (Figure 11C). Filament Width (FW) was the only character with a distinct vector orientation but had only limited influence on the variation observed (Figure 11C). The overall dominance of PC1 over PC2 suggests that vegetative traits have a greater impact on differentiation than floral traits, which appear more uniform across populations.

Removal of polyploids of ML and KA localities did not significantly change the patterns, with the OM population still being the most distinct (Figure 12C). Diploid plants from NI locality ($2n = 2x = 14$) were closer to the IM and PE ($2n = 2x = 12$), a relationship that became even more apparent when bulb size was excluded from the analysis (Figure 12D). The latter two also exhibited the highest overlap. Furthermore, the two allotetraploid populations, ML and KA, were distinctly separated and their differentiation was not influenced by bulb size when analysed together (Figure 12E, F). The final analysis, excluding the OM and NI populations (both $2n = 2x = 14$), showed considerable overlap among populations IM, PE (both $2n = 2x = 12$) and KA (Group I allotetraploids $2n = 4x = 25, 26, 27$), whereas ML was clearly separated.

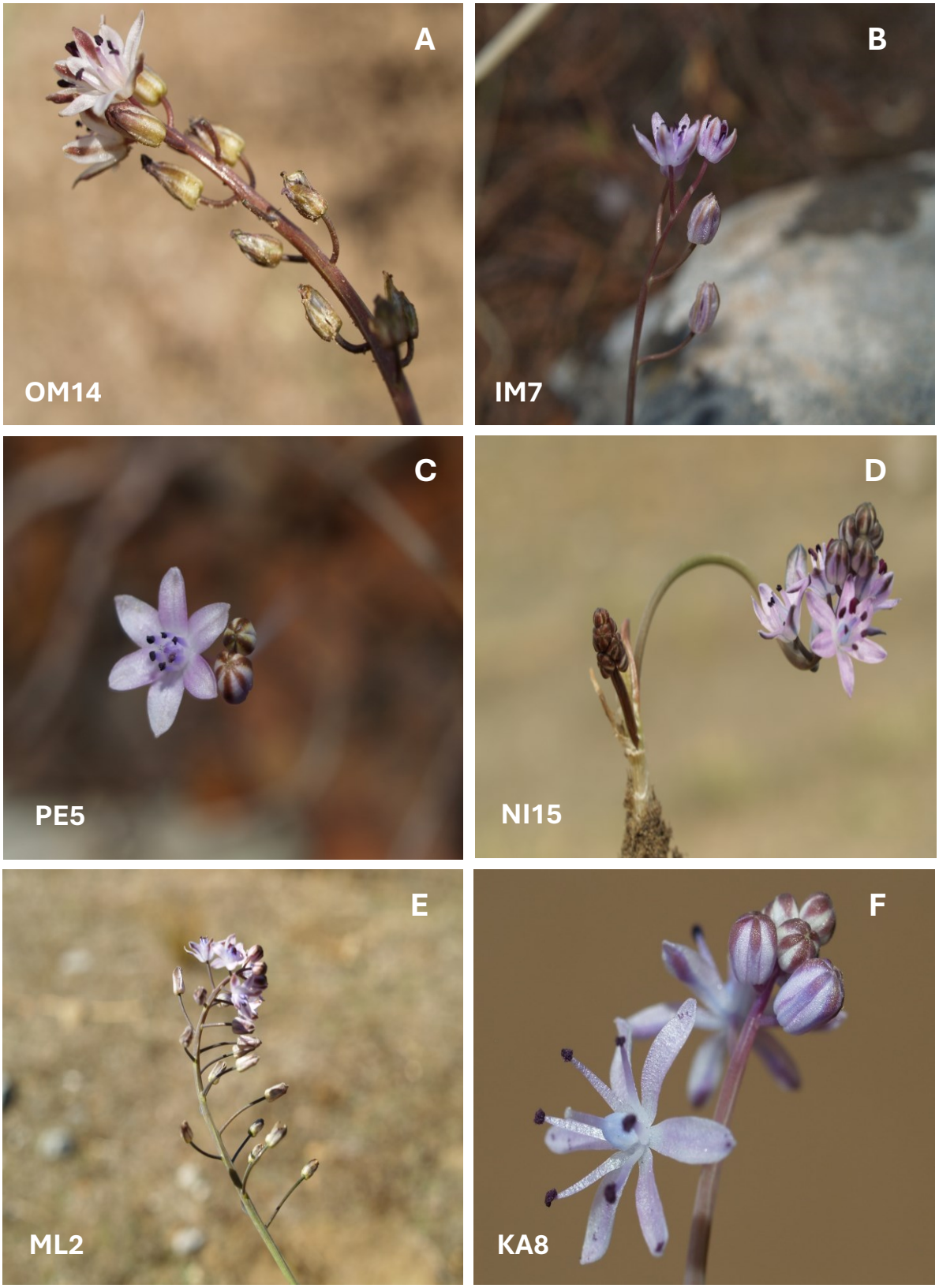

Figure 10. Inflorescences of representative individuals from each locality, photographed in the wild on the day of collection. A) Individual OM14; B) Individual IM7; C) Individual PE5; D) Individual NI15; E) Individual ML2; F) Individual KA8.

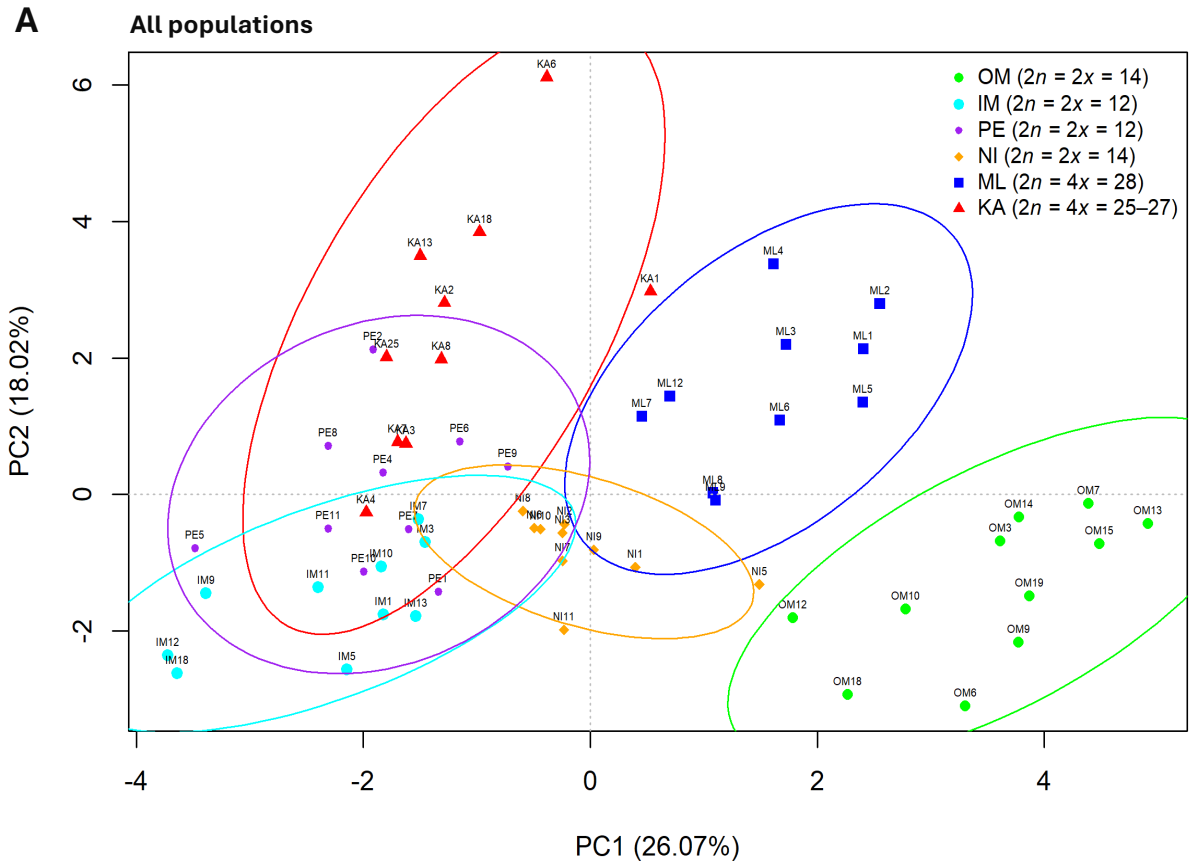

B

No.	Character	Abb.
1	Leaf length	LL
2	Leaf width	LW
3	Number of leaves	NoL
4	Bulb length	BL
5	Bulb width	BW
6	Inflorescence length	IL
7	Number of inflorescences	NoF
8	Pedicel length	PL
9	Number of flowers	NoF
10	Tepal length	TL
11	Tepal width	TW
12	Filament length	FL
13	Filament width	FW
14	Anther length	AL
15	Anther width	AW
16	Ovary length	OL
17	Ovary width	OW
18	Style length	SL
19	Style width	SW

C

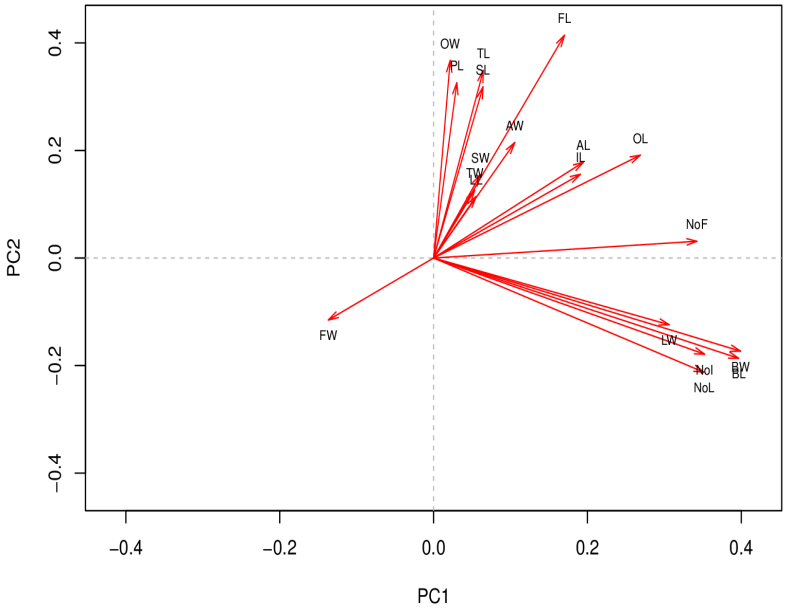

Figure 11. Principal Component Analysis (PCA) of all morphometric data for all characters. A) PCA of all populations based on analyses of all characters, including bulbs; B) List of all 19 morphological characters used for the analysis and their abbreviations; C) Eigenvectors of the two principal components for the "All populations" analysis.

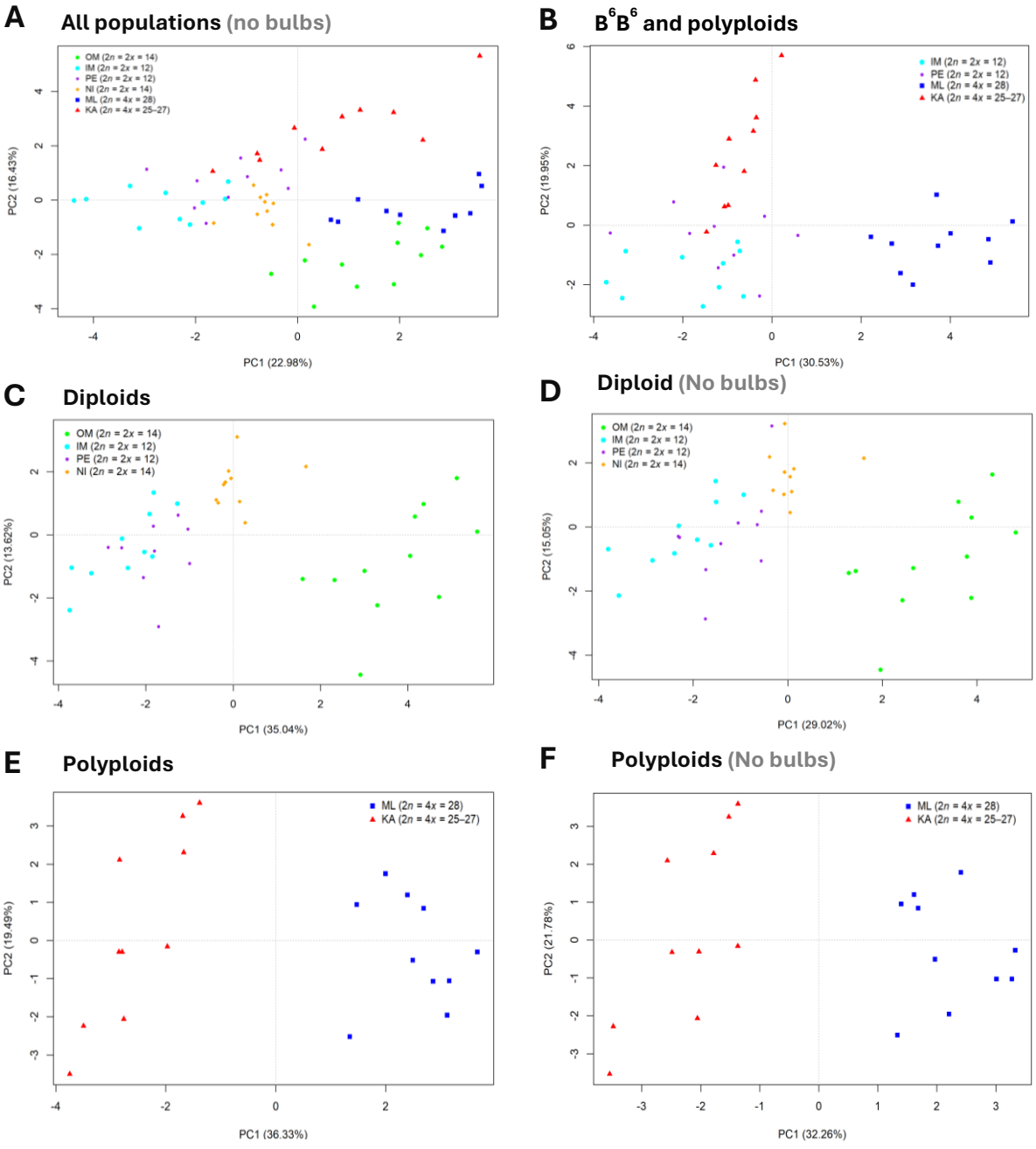

Figure 12. Principal Component Analysis (PCA) of subsets of morphometric data. A) PCA of all characters, except for bulbs, of all analysed populations ; B) PCA of diploid B^6B^6 cytotypes (populations IM and PE) and two polyploid populations (KA and ML); C) PCA of all characters, including bulbs, of diploid B^7B^7 (OM and NI) and B^6B^6 (IM and PE) populations; D) PCA of all characters, excluding bulbs, of diploid B^7B^7 (OM and NI) and B^6B^6 (IM and PE) populations; E) PCA of all characters, including bulbs, of two polyploid populations, KA and ML; F) PCA of all characters, excluding bulbs, of two polyploid populations, KA and ML.

(Figure 12B). This pattern was also evident in the 'All populations (no bulbs)' analysis, where ML locality was in closer proximity to NI and OM plants (both $2n = 2x = 14$; Figure 12A).

Intra- & interpopulation variation and comparison with original descriptions

All morphological traits (except for anther length and width) were analysed individually using comparative boxplots to assess intrapopulational variation and allow for interpopulational comparisons (Figure 13). Additionally, the values for all these characters provided in the original species descriptions (Speta, 2000) were added in order to evaluate the consistency of morphological variation over time and to validate the significance of each character. Intrapopulational variation was consistently present but moderate. Allotetraploid populations ML and KA exhibited a broader range of trait values, though this varied across characters. Although the comparison of various characters revealed substantial differences between populations, these were only specific for the individual traits or traits groups. Thus, no specific overall pattern emerged. All individuals from OM population ($2n = 2x = 14$) had clearly distinct (larger) bulb size, leaf width, number of leaves, and inflorescences, but their floral traits overlapped considerably with the other populations, except for pedicel length (Figures 13A, B, D-F, N). The allotetraploid Group II population ML had the longest pedicels and narrowest filaments (Figures 13H, N), but its other traits were similar to all other examined plants. Even within cytotypes, there was no general consistency of character combinations. All diploid IM and PE (both $2n = 2x = 12$) individuals consistently had the shortest filaments and fewest flowers (Figures 13G, Q), but differed in leaf length (Figure 13C), with IM population having consistently the shortest leaves of all samples. These also shared the narrowest leaves with the two allotetraploid populations, ML and KA (Figure 13D), and the smallest bulb sizes with Group I allotetraploid population KA (Figures 10F, 13A, B). Floral architecture was largely consistent across populations, with the exception of the majority of KA plants, which had narrower and elongated tepals (Figures 13I, J), although the values were still overlapping with the other populations.

Comparison of the morphological characters analysed in the current study with those of the original species descriptions broadly indicated consistency and thus stability of the characters. In most cases, the observed ranges of the trait values were similar or at least followed the same trend, with some exceptions. Overall, vegetative traits were largely consistent with the original data. Floral traits, however, displayed greater and often consistent differences. Diploid B^7B^7

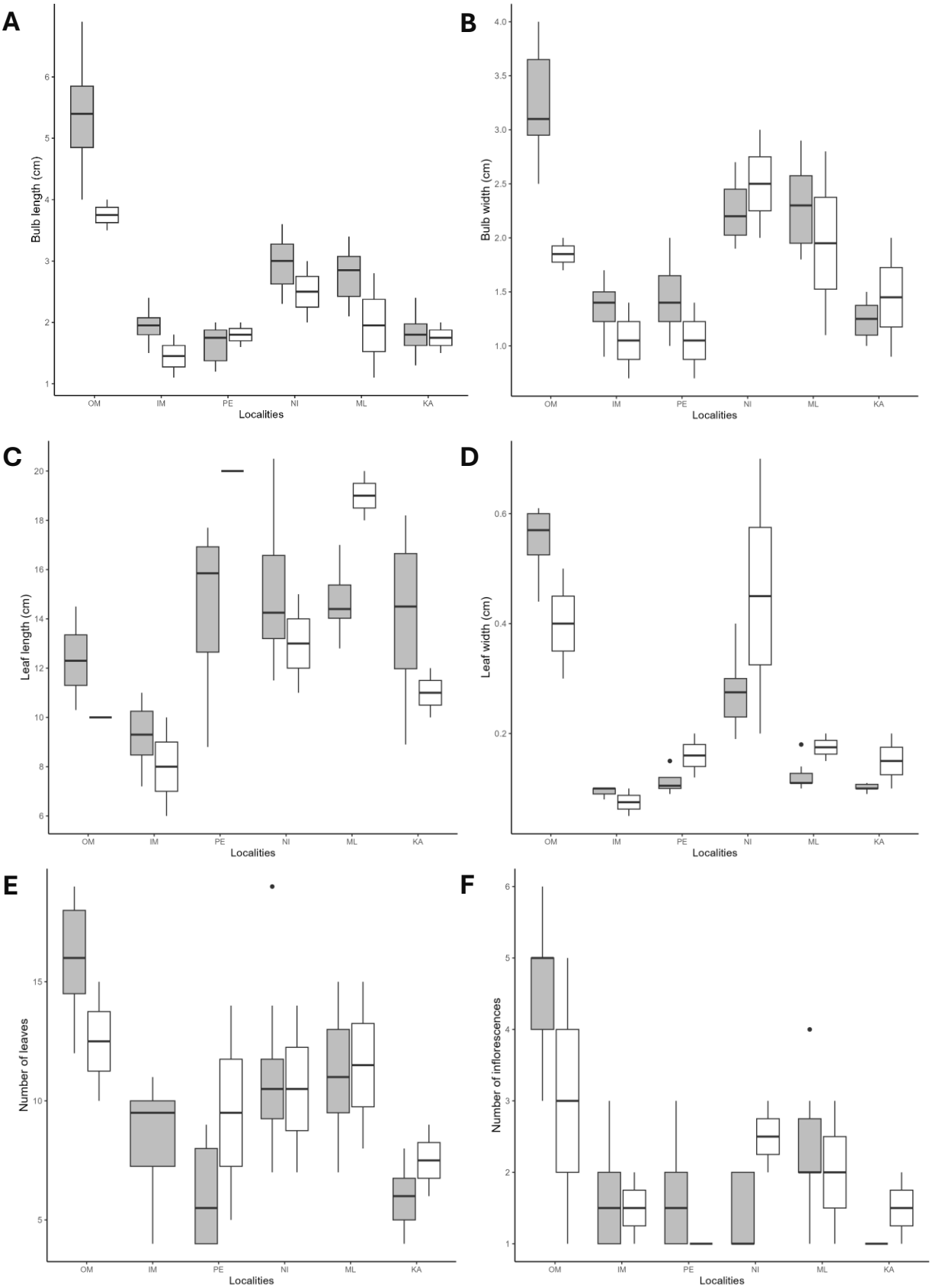

Figure 13. Comparison of variation of individual morphological characters analysed in this study (grey) with the characters of the original descriptions (white) for individuals of the six type localities. A) Bulb length; B) Bulb width; C) Leaf length; D) Leaf width; E) Number of leaves; F) Number of inflorescences.

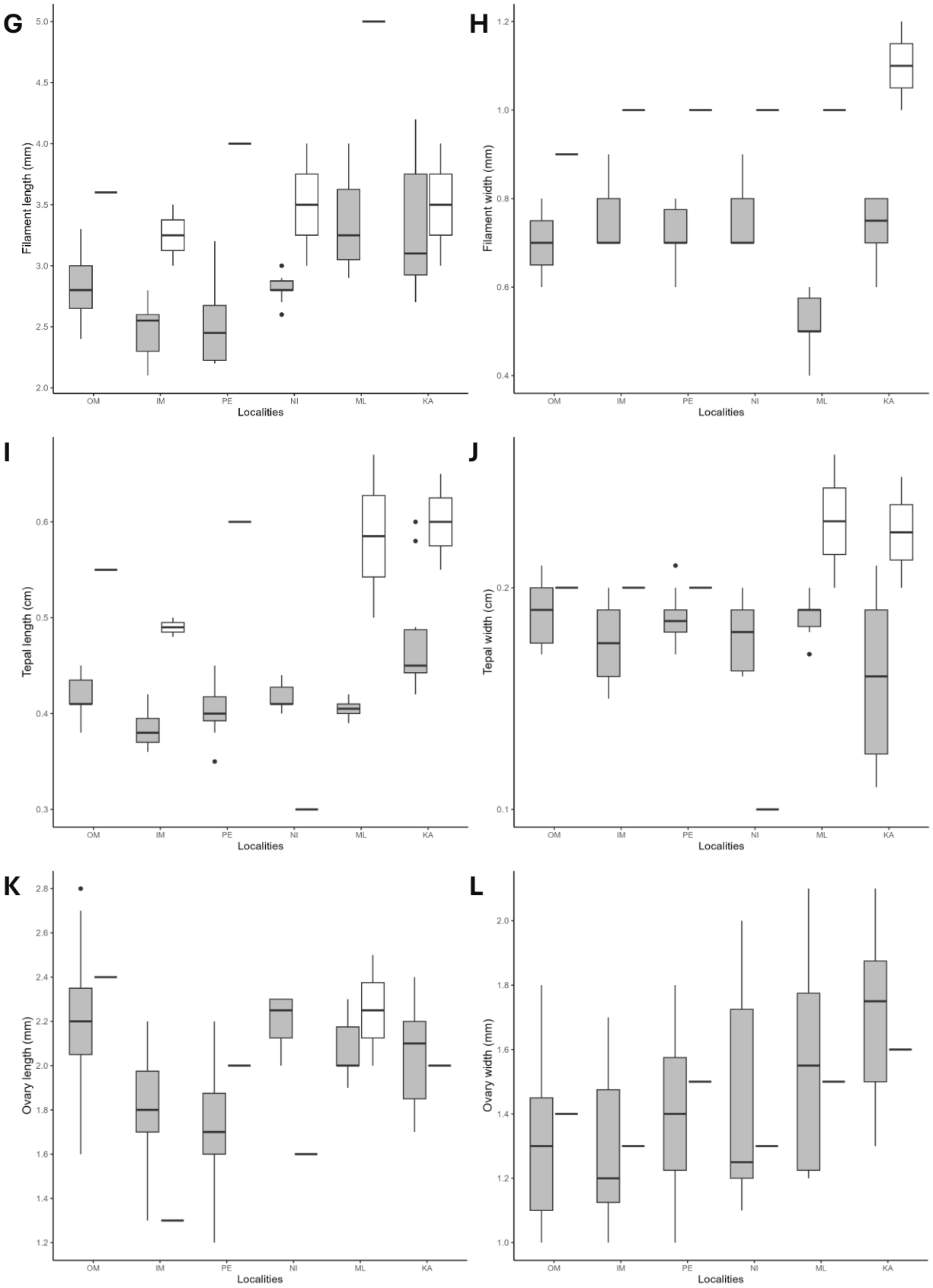

Figure 13. (continued) Comparison of variation of individual morphological characters analysed in this study (grey) with the characters of the original descriptions (white) for individuals of the six type localities. G) Filament length; H) Filament width; I) Tepal length; J) Tepal width; K) Ovary length; L) Ovary width.

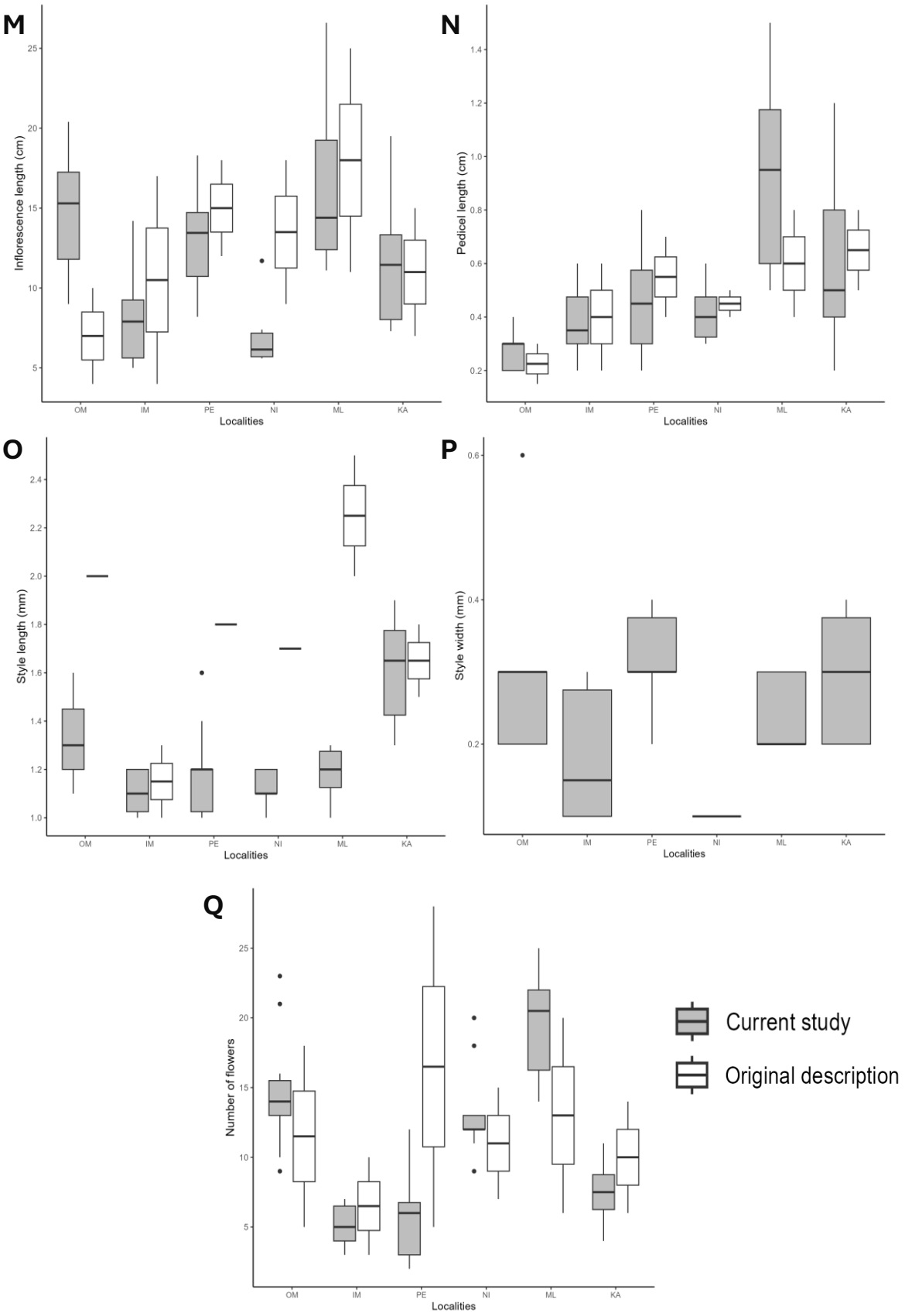

Figure 13. (continued) Comparison of variation of individual morphological characters analysed in this study (grey) with the characters of the original descriptions (white) for individuals of the six type localities. M) Inflorescence length; N) Pedicel length; O) Style length; P) Style width; Q) Number of flowers.

population OM had notably larger bulbs and leaves (Figure 13A, B), and slightly higher number of flowers and inflorescences compared to original species description (Figures 13F, Q). In contrast, plants from the other B^7B^7 diploid NI population had narrower leaves and shorter inflorescences (Figures 13D, M). Allotetraploids of Group II (ML population) had shorter leaves and style, but a higher number of flowers (Figures 13C, O, Q) and diploid B^6B^6 plants from PE locality differed significantly in the number of flowers and leaf length (Figures 13C, Q). Overall, diploids B^6B^6 (IM population) and allotetraploids of Group I (KA population) were the most consistent with their original descriptions.

Phylogenetic analysis

ITS1+2 regions of three individuals from each of six examined populations were analysed phylogenetically together with previously published sequences (Jang, 2013; Jang et al., 2013) representing 40 diploid and tetraploid individuals from multiple chromosomal races of the genus *Prospero* Salisb. The analysed spacer regions ranged from 641 to 649 base pairs in length. Within the *Prospero autumnale* complex, only substitutions were observed, whereas indels were found exclusively in the main outgroup species, *Othocallis siberica* (Andrews) Speta, and in the two species outside the *Prospero autumnale* complex, *Prospero obtusifolium* (Poir.) Speta and *Prospero hanburyi* (Baker) Speta.

The resulting Maximum Likelihood (ML) phylogenetic tree recovered the *Prospero autumnale* complex as a distinct lineage, supported by a bootstrap value (BS) of 82. Within this complex, three major Clades were identified. Clade I comprised B^6B^6 diploids together with Group I and Group II $B^6B^6B^7B^7$ allotetraploids (BS 81), Clade II included the AA diploid cytotype (BS 100) and Clade III encompassed B^7B^7 diploids, allotetraploids AAB^7B^7, and Group II, III and IV $B^6B^6B^7B^7$allotetraploids (BS 91; Figure 12) All examined individuals from the populations IM, PE (both B^6B^6), ML (Group II, $B^6B^6B^7B^7$ allotetraploids) and KA (Group I, $B^6B^6B^7B^7$ allotetraploids) were recovered in Clade I whereas all plants from OM and NI (both B^7B^7) were placed in Clade III.

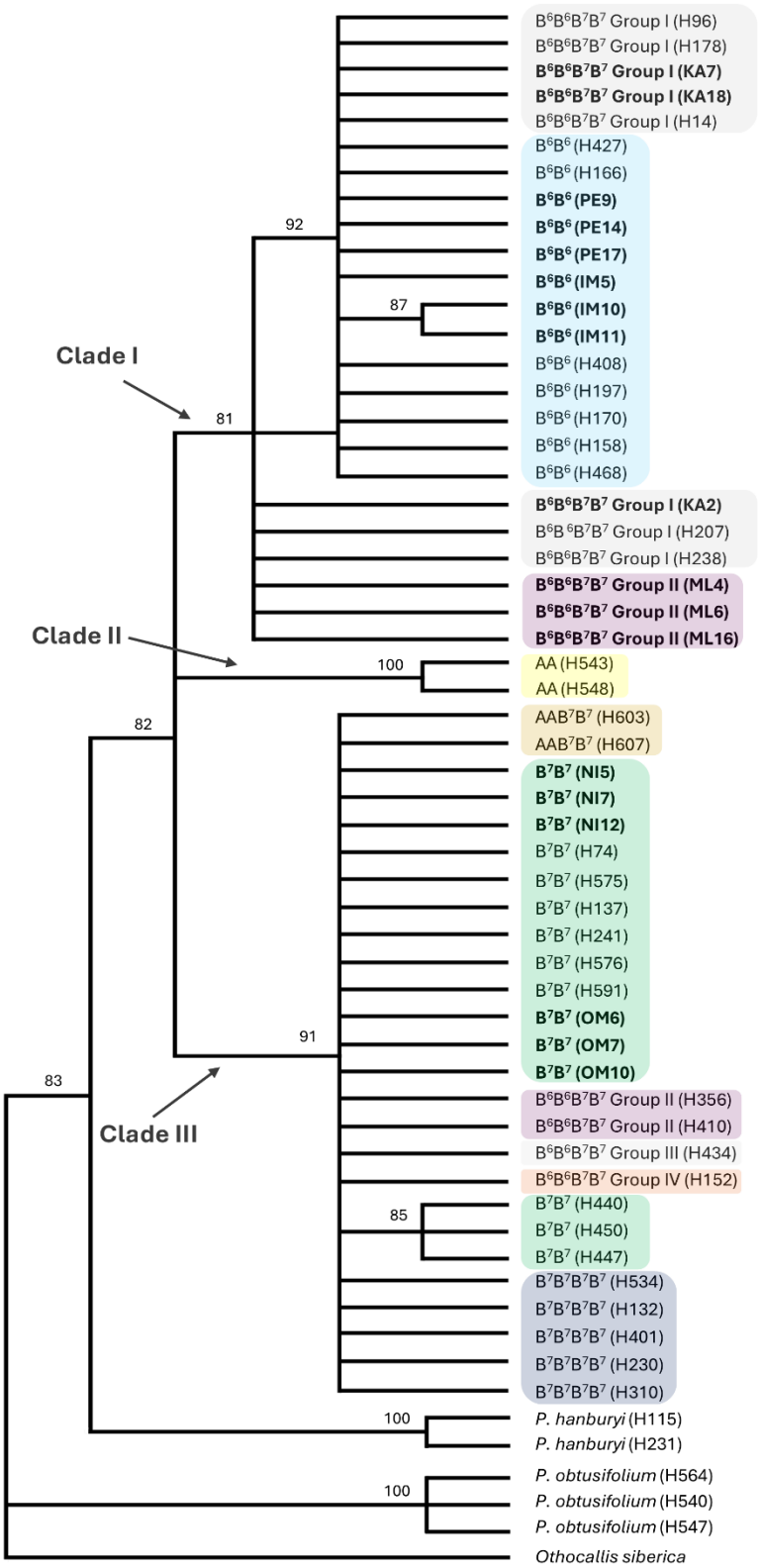

Figure 14. Phylogenetic relationships of 18 individuals representing six analysed populations inferred from ITS sequence data. The currently studied individuals (bold) were analysed together with previously obtained ITS regions of all basic *Prospero autumnale* complex cytotypes (Jang et al., 2018a). Bootstrap support values are indicated above branches. Information on genome composition (coloured; except for outgroups) and plant number (in brackets) is provided for each analysed individual. Diploids of AA indicated in yellow, diploids of B^6B^6 in light blue, diploids of B^7B^7 in green, allotetraploids of AAB^7B^7 in brown, allotetraploids of B^6 and B^7 in grey (Group I), purple (Group II), light grey (Group III), and pink (Group IV), autotetraploids $B^7B^7B^7B^7$ in blue. Arrows indicate the three supported Clades.

Discussion

Karyological diversity

Recent extensive studies on the dynamic genomic nature of *Prospero autumnale* complex have significantly expanded our understanding of chromosomal variation in this species complex. Research has clarified the evolutionary relationships among the four basic diploid cytotypes of the complex (Jang et al., 2013), as well as the evolutionary pathways, genomic features, and chromosomal dynamics, particularly of the allotetraploid races found on Crete (Jang et al., 2018a). These studies have also shed light on the origin and role of supernumerary chromosomes (Jang et al., 2016) and chromosomal segments (Jang et al., 2018b). Given the evidence of genomic complexity and the role it plays in shaping distinct cytotypes across the complex's distribution range, it was essential to re-evaluate the basic karyological data associated with each of the many endemic species that has been described within the complex (e.g., Tzanoudakis & Kypriotakis, 1998; Speta, 2000). The original descriptions of these species did include chromosome numbers, but usually only from only one to few individuals per locality, without accompanying genome size measurements to complete their cytotaxonomic profiles. The current study focused on the six validly described *Prospero autumnale* endemic species on the island of Crete. The sampling was extended to 20 individuals per *locus classicus* of each species. Genome sizes and/or chromosome numbers were established for most of these individuals and the resulting data offered valuable insights into the genomic identity of these populations in the context of known levels of variation reported for Cretan *Prospero autumnale* individuals, especially for allotetraploid populations.

Chromosome numbers and karyotype morphology

Individuals within each examined population/species represented uniformly single cytotype in general agreement with the original species descriptions, with some notable exceptions. *Prospero rhadamanthi* Speta from PE locality has been described possessing $2n = 2x = 14$ (Speta, 2000), but all eight examined individuals from this population were found to possess only $2n = 2x = 12$ chromosomes, thus representing cytotype B^6B^6, and not the originally identified cytotype B^7B^7. This suggests the occurrence of a mixed population in this area, perhaps occupying different microniches/patches along the gorge. A second deviation from expectation was recorded from the KA population, type locality of *Prospero hierapytnense*

Speta. This species has been described as having $2n = 4x = 26$ chromosomes (Speta, 2000). However, among the four examined individuals, three chromosome numbers were found: $2n = 4x = 25$, 26 and 27. It was to be expected considering that plants with $2n = 4x = 26$ chromosomes represent the Group I which can possess $2n = 4x = 25, 26, 27$ or 28 chromosomes while being genetically balanced. This is due to the meiotic pairing of the large sub-metacentric chromosome F^1(6-7) and its homoeologous free chromosomes 6 and 7 as either bivalents, resulting in meiotic products possessing $n = 12$ chromosomes, or as trivalents [F^1(6-7)+6+7] resulting in haploid cells with $n = 12$, 13 or 14 chromosomes (Jang et al., 2018a). Therefore, formally, only individuals of this population possessing $2n = 4x = 26$ can be identified as *Prospero hierapytnense* Speta. Such variation in the chromosome numbers violates a foundamental formal prinicples of the species concept. Nevertheless, as a population, the plants were genomically all belonging to Group I and small adjustment to species description would correct the inconsistency.

The four remaining examined populations were chromosomally consistent with the original species descriptions (Speta, 2000). Their basic karyotypes also corresponded well to the recently characterized karyotypes of all diploid and tetraploid cytotypes in terms of chromosome number, centromere positions of all chromosomes, and Nucleolus Organizer Region (NOR) locations. Specifically, the karyotypes of individuals from the OM and NI localities corresponded to the B^7B^7 cytotype, while those from IM and PE to the B^6B^6 cytotype. Plants from the ML locality with $2n = 4x = 28$ chromosomes could not be assigned to any specific Group of allotetraploids based solely on karyotype since all four distinct allopolyploid Groups from Crete share this chromosome number (Jang et al., 2018a). The presence of two chromosomes of the same size of each chromosome type, however, suggested their assignment to Group II allopolyploids.

The supernumerary chromosomal segments and B chromosomes found in three individuals have been reported before in nearly all cytotypes and were suggested to represent remnants of chromosomal rearrangements rather than conserved features specific to particular populations (Jang et al., 2016, 2018b). It is therefore also likely that additional B chromosomes exist in other individuals from the IM population or other localities not captured in the current sampling. Terminal supernumerary segments, found on different chromosomes in two individuals from the KA locality, represent most likely more ancient translocations of Bs or other chromosomal segments that are shared by different cytotypes (Jang et al., 2018b).

Genome size diversity

Genome sizes were measured for the first time for the six populations representing six endemic *Prospero* Salisb. species in their six *loci classici*. A population originating from the Ida Mountains, where the NI locality is also situated, was previously reported to have a genome size of 4.73 pg/1C (Ebert et al., 1996). However, due to the lack of precise coordinates, it remains unclear whether this measurement corresponds to the type locality of *Prospero idaeum* Speta (Speta, 2000). Within each of the six populations studied here, genome size values were uniform, without any exception, with only slightly higher levels of variation observed in the polyploids. The presence of the B chromosome in the individual IM15 was followed by a minimal increase in genome size compared to the rest of the individuals of this population.

The observed genome sizes of each population corresponded well to the known cytotypes (Jang et al., 2013, 2018b). All individuals from the NI locality exhibited DNA content consistent with the standard B^7B^7 cytotype, more closely resembling Type II (Jang et al., 2013). The genome sizes of populations IM and PE corresponded to the B^6B^6 cytotype. Genome sizes of all examined allotetraploid KA plants corresponded to genome size ranges of Group I $B^6B^6B^7B^7$ allotetraploids, as suggested also by the variable chromosome numbers. The other allotetraploid population from ML locality possessed a genome size indicative of Group II allotetraploids of Crete, as suggested by the karyotype morphology (Jang et al., 2018a). Finally, genome size values of the OM population corresponded to the B^7B^7 cytotype, albeit were slightly higher and more similar to the previously mentioned Ida Mountains population (Ebert et al., 1996).

For several individuals, both genome size and chromosome number were determined, allowing for direct correlation of these two parameters and completing their genomic profiles. Given the consistency observed in both parameters within populations, a uniform cytotype has been inferred for each analysed locality. Chromosome number, karyotype morphology, and genome size data together supported the assignment of each population to previously established cytotypes. The new data fit perfectly into the previously published model of cytotype diversification in Cretan *Prospero autumnale* complex (Jange et al., 2013, 2018a) and allowed us to conclude that the collected populations are not defined by novel structural genomic characters that would support their status as distinct evolutionary genomic units.

Mapping of two satellite DNAs in the allotetraploid populations

The formation of allotetraploids on the island of Crete appeared to follow a two-step process. Primary allotetraploids (not found), that arose from hybridization between the B^6B^6 and B^7B^7 diploids, underwent subsequent backcrosses in various configurations leading to the emergence of three secondary allotetraploid groups. The number and localization of the *PaB6* satellite loci have been shown to allow for identification of all four main $B^6B^6B^7B^7$ lineages (Emadzade et al., 2014). Thus, to clarify the evolutionary origins of the tetraploid populations from KA and ML localities, the *PaB6* repeat was mapped in chromosomes of selected individuals. The presence of 26 pericentric *PaB6* signals in individual KA5 allowed its unambiguous assignment to Group I allotetraploids, in agreement with the variable chromosome numbers of $2n = 4x = 25\text{-}27$ and the genome size values. In contrast, only 14 of 28 chromosomes of ML population carried *PaB6* loci in all three individuals examined, again allowing unambiguous assignment of this population to Group II allotetraploids, consistent with the measured genome size values (Jang et al., 2018a).

This study represents the first systematic attempt to assess the levels of uniformity within diploid and allotetraploid *Prospero autumnale* complex populations. Previous research often lacked either precise sampling data of the individuals analysed and/or did not use populational sampling (Ebert et al., 1996; Jang, 2013) The data obtained in the current study strongly suggest that each of the four allotetraploid Groups on Crete may be locally established and homogeneous. However, broader sampling across populations is needed, not only to confirm this pattern but also to test whether potential genetic isolation underlies the distribution of these allotetraploid cytotypes.

Morphological variation within *Prospero autumnale* complex in Crete

Interpretation of morphometric data

Despite the generally low degree of morphological differentiation indicated in the original species descriptions (Table 1), the results of the morphometric analysis revealed that a certain level of structured morphological differentiation exists among the populations collected from the type localities of the six endemic *Prospero* Salisb. species in Crete. These findings are consistent with both field observations and *ex situ* cultivation data, as each population displayed a distinct and consistent timing of leaf emergence. However, there is still a high degree of morphological overlap between populations that makes the construction of a reliable identification key based solely on morphology challenging.

Cytological profiling of each population allowed their assignment to known cytotypes and exploring the relationship between their cytological characters and morphology. Analysis restricted to diploid cytotypes showed that the OM population (B^7B^7, $2n = 2x = 14$) was most differentiated from the rest of the analysed localities. The other B^7B^7 cytotype population from NI was morphologically more similar to the two B^6B^6 populations, despite their different cytogenetic profile, than to the B^7B^7 OM population. The two B^6B^6 populations, in contrast, exhibited more considerable morphological similarity.

The two allotetraploid populations analysed alone were clearly distinct from one another. However, when analysed together with B^6B^6 populations, the Group I allotetraploid population KA clustered closely with the B^6B^6 populations, while the Group II allotetraploid population ML appeared as a distinct and isolated cluster. This pattern has also been observed in larger datasets (Jang, 2013). Genomic *in situ* hybridization (GISH) data suggested that the genome of Group I allopolyploids has become homogenized toward the B^6 maternal genome, supporting the observed morphological similarity (Jang et al., 2018a). Similarly, the origin of Group II allotetraploids as backcrosses between Group I and the B^7B^7 original paternal cytotype, is consistent with the morphological similarity of the ML population with B^7B^7-like traits. In both cases, cytogenetic background appears to be reflected in the morphological characteristics. These general patterns were also observed when all populations were analysed together, although the level of overlaps was higher. Morphological population/species delimitation became even more difficult when bulb characters were excluded from the analysis. These characters were excluded because bulb morphology could potentially correlate more significantly with the age of the individual than with stable, genome-related traits, and thus may not reliably reflect taxonomic differences.

The analysis of intra- and interspecific variation of the six analysed populations also enabled evaluation of each morphological character and its potential diagnostic value. Several characters were of high relevance for defining OM population (B^7B^7, $2n = 2x = 14$) as a distinct group compared with the other examined populations. Despite this, morphological characters, even when considered alongside cytological data, often fell within overlapping ranges across populations, limiting their effectiveness in clearly separating each population. For example, leaf width was consistently below 0.11 mm in all individuals within B^6B^6 and Group I cytotypes, as also noted earlier (Jang, 2013). This suggests that plants with wider leaves likely belong to B^7B^7 or other allotetraploid groups. However, narrower leaves are not exclusive to the B^6B^6 cytotype, as some B^7B^7 individuals have also shown similar traits.

Flower number also emerged as a potentially useful distinguishing character since the B^6B^6 populations from PE and IM consistently had fewer than seven flowers, while the allotetraploid population ML had more than sixteen. However, earlier studies reported B^6B^6 plants with higher flower counts, indicating character overlap within the same cytotype, but across the populations. Certain traits stood out as more significant in explaining the variation than others, as evidenced by the eigenvectors extracted from the PCA. However, not all traits that seemed important in the field contributed strongly to the PCA results. Floral and vegetative traits each formed distinct groups with similar eigenvector orientations within their respective sets, suggesting that traits within each group may co-evolve and be influenced by shared factors. Overall, no single character proved consistently diagnostic, but instead, combinations of characters defined population-level variation. Each population appeared to be distinguishable by a unique set of traits, but overlapping values prevented the formulation of a practical identification key, complicating efforts at reliable classification. This may explain why morphotypes described as species from Crete have not been validly documented elsewhere on the island.

Endemic species vs. uniform cytotype populations

Comparison of the current data with the original species descriptions (Speta, 2000) indicated general consistency in character ranges, with notable exceptions. One of the most prominent differences concerned floral characters with values much higher in the current study. This may reflect differences in methodology, as the original measurements were likely taken from fresh material, whereas the current study used dried specimens. The most evident differences were found in tepal and filament dimensions, while style and ovary measurements showed irregular inconsistencies. All the measurements for the current study were made under similar drying conditions and therefore should be comparable within this study. Population PE exhibited the greatest morphological divergence from original descriptions, likely due to a difference in chromosome number of all plants collected for this study (B^7B^7, $2n = 2x = 14$) and plants originally described (B^6B^6, $2n = 2x = 12$). This finding highlights the extent of variation that can exist between nearby populations or even plants of the *Prospero autumnale* complex, especially when considering that plants do not reproduce asexually. The collected population was the only one growing there at the date of collection, beginning of October of 2024, and was found in an altitude of 50m. A survey conducted later in the same month revealed a great number of individuals possessing sets of characters that more closely resembled the B^7B^7 species described for that locality growing in the entrance of the gorge, closer to the sea level

(M. Choreftakis pers. comm.). Hence, it is hypothesized that phenological differences between cytotypes may contribute to reproductive isolation and multiple cytotypes can co-exist at a given locality. Thus, repeated sampling at different times during the flowering period of *Prospero autumnale* (September to late November), is certainly crucial for a better understanding of populations complexity. Lastly, qualitative traits from the original descriptions were also recorded but not analysed here in detail, having been estimated to be of limited taxonomic value (preliminary data). Additionally, given the relatively short timespan since the original descriptions (~30 years), long-term morphological shifts cannot be confidently inferred.

Morphometric analyses confirmed the presence of structured, yet overlapping, variation among the six studied populations. When interpreted alongside cytogenetic data, some correlation between the cytotype and morphology could be inferred, though not consistently. Analyses of more individuals, especially from the allotetraploid Groups, would likely increase observed overlap due to continuous character variation. Although some morphological structuring was evident and might relate to cytotype, morphology alone is insufficient for robust species delimitation in the *Prospero autumnale* complex on Crete. As such, any formal taxonomic treatment remains uncertain when based solely on the morphology.

Habitat and cytotype

Habitat can potentially influence morphology, resulting in diversification of ecotypes rather than distinct species. Although no standardized ecological data were collected during sampling, relevant general habitat observations were recorded and considered. The IM, PE (both B^6B^6), and KA (Group I, $B^6B^6B^7B^7$) populations were all located in gorges with similar environmental conditions, representing typical habitats for Crete. These populations were found in relatively undisturbed and isolated patches along the inner parts of these gorges. Similarly, the ML population (Group II, $B^6B^6B^7B^7$), despite occurring at a much higher altitude, was situated at the entrance of a gorge in equally intact terrain. The plateau associated with the type locality is considerably larger, and it is likely that the individuals used in the original species description were collected from a different part of this area than those sampled in the present study. Given the plateau's size and the fact that the population sampled here represented an allotetraploid cytotype attributed to the presumed local species, it is highly probable that a large polyploid population is established in this region. Notably, despite previous extensive sampling (Taylor, 1997), polyploid individuals have only been documented from the eastern part of Crete, raising questions about the adaptability of these cytotypes to the region’s drier climate and their

successful establishment. Of the two B^7B^7 populations, the NI population was found on the highest plateau in Crete and its type locality was the only one defined with exact geographic coordinates. Although the plateau spans several square kilometers, all observed individuals were confined to the specific small area referenced in the original description. The reason for this restricted distribution, despite broader suitable habitat nearby, remains unclear. The most ecologically distinct site was found near the seasonal lake at the OM (B^7B^7) locality, characterized by periodic flooding. This may explain the consistent presence of certain traits in this population, such as larger bulbs, broader leaves, and a higher number of inflorescences, possibly reflecting habitat-driven morphological adaptation. Overall, these observations highlight the importance of integrating ecological data to cytogenetic and morphological analysis to better understand the phenotypic variability within the *Prospero autumnale* complex in Crete. A future study explicitly combining environmental parameters, cytogenetics, genetics, and morphology is critical for clarifying the role of habitat in shaping this cytological and morphological variation.

Phylogenetic inferences

The phylogenetic relationships within the genus *Prospero* Salisb., and particularly among the cytotypes of the *Prospero autumnale* complex, have been previously examined by Jang et al. (2013, 2018a). These studies consistently showed that, based on analyses of ITS1+2 and some plastid markers, diploid cytotypes form distinct clades, while the inclusion of polyploids introduced topological ambiguity. The results of the present study conform to these earlier findings, since all six examined populations were recovered within corresponding lineages.

The three analysed allotetraploid KA individuals (Group I) clustered together with B^6B^6 diploids and the previously analysed Group I allotetraploids in Clade I. The three allotetraploid ML individuals (Group II) were also recovered in the same clade. In contrast, the two previously analysed Group II plants were instead placed within Clade III. These placements are consistent with morphological and genomic patterns identified in prior morphometric and genomic analyses, which suggested a close relationship between Group I and its maternal B^6B^6 cytotype (Jang et al., 2018a). Group II was inferred to originate from backcrosses involving Group I plants with $2n = 4x = 28$ chromosomes and diploids of B^7B^7, albeit crosses in both directions were identified (Jang et al., 2018a), which is also reflected in the current placement of the five Group II individuals.

In summary, the ITS sequence data did not support phylogenetically distinct status for the six populations analysed in this study. However, this does not preclude the possibility that other genomic differences may exist. Further investigation could allow inference of more structured phylogenetic relationships among *Prospero autumnale* cytotypes.

Conclusions

The multidisciplinary approach used in this study did not conclusively support or contradict current taxonomic treatment for the six endemic species of the *Prospero autumnale* complex from Crete, although it provided valuable insights into the levels of intra- and interpopulational variation. The data particularly have clearly shown that local populations/segregates exhibit combinations of morphological traits that are distinct to a certain extent. Cytological analyses indicated cytotype uniformity within these populations, despite the known cytological diversity in the region. Furthermore, all individuals examined represented previously described chromosomal races, with no evidence of chromosomal differentiation underlying the observed morphological variation, although undetected chromosomal rearrangements cannot be ruled out. Morphometric analyses provided additional evidence for the existence of distinct morphotypes, as shown by population-level morphological clustering and differentiation. However, morphological character combinations and the levels of variation combined with existence of diploid and polyploid cytotypes are not distinct enough to support the taxonomic status of these six species. Phylogenetic analysis grouped the populations according to their cytotypes, in agreement with earlier morphological and cytological data, thus failing to provide support for their recognition as distinct species. Denser sampling and analyses of *Prospero autumnale* on Crete should shed more light on the levels of morphological variation and distinctiveness of populations.

Long-term research on the *Prospero autumnale* complex has allowed for a better understanding of the evolutionary dynamics of its cytotypes. The broader picture points to a model of chromosomally driven diversification, in which genomic plasticity is reflected in chromosomal rearrangements, the presence of recurrently formed B chromosomes and ancient supernumerary segments, has given rise to a range of stable yet evolving entities. Hence, each cytotype may represent a distinct evolutionary unit, but whether such units should be considered separate species remains debatable and depends on the applied species concept. Given that cytotaxonomy alone cannot decisively define taxonomic boundaries within a

complex shaped by such genomic mechanisms, the recognition of locally differentiated morphotypes as distinct taxa appears unjustified. Thus, the integrative interpretation of morphological, cytological, and phylogenetic evidence does not lend unequivocal support for the distinct taxonomic status of the six endemic species from Crete. Rather, the current results indicate a need for revision in favor of lumping over splitting. In-depth understanding of the patterns and processes driving the observed morphological, cytological and ecological differentiation within the *Prospero autumnale* complex on Crete will require more analyses based on broader and denser sampling to reach well-supported taxonomic conclusions.

Literature

Ainsworth CC. (1980) The population cytology of *Scilla autumnalis*. Ph.D. Thesis, University of London, London, UK.

Brullo C, Brullo S, Giusso Del Galdo G, Pavone P, Salmeri C. (2009) *Prospero hierae* (Hyacinthaceae), a new species from Marettimo Island (Sicily). *Phyton* **49**:93–104.

Ebert I, Greilhuber J, Speta F. (1996) Chromosome banding and genome size differentiation in *Prospero* (Hyacinthaceae): Diploids. *Plant Systematics and Evolution* **203**:143–177.

Emadzade K, Jang T-S, Macas J, Kovařík A, Novák P, Parker J, et al. (2014) Differential amplification of satellite *PaB6* in chromosomally hypervariable *Prospero autumnale* complex (Hyacinthaceae). *Annals of Botany* **114**:1597–1608.

Firat M, Yildirim H. (2016) *Prospero cudidaghense* sp. nov. (Asparagaceae): a new species from southeastern Anatolia, Turkey. *Turkish Journal of Botany* **40**: Article 5.

Govaerts, R. (2015) World Checklist of Selected Plant Families. Royal Botanic Gardens, Kew.

Greilhuber J, Ebert I. (1994) Genome size variation in *Pisum sativum*. *Genome* **37**:646–655.

Jang T-S. 2013. Chromosomal evolution in *Prospero autumnale* complex. PhD thesis, University of Vienna, Vienna, Austria.

Jang T-S, Emadzade K, Parker J, Temsch EM, Leitch AR, Speta F, et al. (2013) Chromosomal diversification and karyotype evolution of diploids in the cytologically diverse genus *Prospero* (Hyacinthaceae). *BMC Evolutionary Biology* **13**:136.

Jang T-S, Parker J, Weiss-Schneeweiss H. (2016) Structural polymorphisms and distinct genomic composition suggest recurrent origin and ongoing evolution of B chromosomes in the *Prospero autumnale* complex (Hyacinthaceae). *New Phytologist* **210**:669–679.

Jang T-S, Parker JS, Emadzade K, Temsch EM, Leitch AR, Weiss-Schneeweiss H. (2018a) Multiple origins and nested cycles of hybridization result in high tetraploid diversity in the monocot *Prospero*. *Frontiers in Plant Science* **9**:433.

Jang T-S, Parker JS, Weiss-Schneeweiss H. (2018b) Euchromatic supernumerary chromosomal segments—remnants of ongoing karyotype restructuring in the *Prospero autumnale* complex? *Genes* **9**:468.

Jang T-S, Weiss-Schneeweiss H. (2015) Formamide-Free Genomic *in situ* Hybridization Allows Unambiguous Discrimination of Highly Similar Parental Genomes in Diploid Hybrids and Allopolyploids. *Cytogenetic and genome research* **146** (4): 325–331.

Kumar S, Stecher G, Li M, Knyaz C, Tamura K. (2023) MEGA12: Molecular Evolutionary Genetics Analysis version 12. *Molecular Biology and Evolution* **40**:1593–1596.

Otto FJ, Oldiges H, Goehde W, Jain VK. (1981) Flow cytometric measurement of nuclear DNA content variations as a potential in vivo mutagenicity test. *Cytometry* **2**:189–191.

Parker JS, Lozano R, Taylor S, Ruiz Rejón M. (1991) Chromosomal structure of populations of *Scilla autumnalis* in the Iberian Peninsula. *Heredity* **67**:287–297.

Rukšans J. (2007) *Buried Treasures: Finding and Growing the World's Choicest Bulb*. Portland, OR, USA: Timber Press.

Speta F. (1982) Die Gattungen *Scilla* L. s. str. und *Prospero* Salisb. im pannonischen Raum. *Veröffentlichungen der Internationalen Clusius-Forschungsgesellschaft Güssing* **5**:1–19.

Speta F. (1998). Systematische Analyse der Gattung *Scilla* L. s.l. (Hyacinthaceae). *Phyton (Horn)* **38**(1): 1–141.

Speta F. (2000) Beitrag zur Kenntnis der Gattung *Prospero* Salisb (Hyacinthaceae) auf der griechischen Insel Kreta. *Linz Biologische Beiträge* **32**:1323–1326.

Tamura K, Nei M. (1993) Estimation of the number of nucleotide substitutions in the control region of mitochondrial DNA in humans and chimpanzees. *Molecular Biology and Evolution* **10**:512–526.

Taylor S. (1997) Chromosomal evolution of *Scilla autumnalis*. Ph.D. Thesis, University of London, London, UK.

Temsch E, Greilhuber J, Krisai R. (2010) Genome size in liverworts. *Preslia* **82**:63–80.

Tzanoudakis D, Kypriotakis Z. (1998) A new polyploid *Scilla* (Liliaceae) from the Cretan area (Greece). *Folia Geobotanica* **33**:103–108.

Vaughan HE, Taylor S, Parker JS. (1997) The ten cytological races of the *Scilla autumnalis* species complex. *Heredity* **79**:371–379.

Vestek A, Slovák M, Weiss-Schneeweiss H, et al. (2019) Morpho-anatomical differentiation and genome size variation in three ploidy levels within the B7 cytotype of *Prospero autumnale* (Hyacinthaceae) complex from the Balkan Peninsula and Pannonian Basin. *Plant Systematics and Evolution* **305**:597–609.

Weiss-Schneeweiss H, Emadzade K, Jang T-S, Schneeweiss GM. (2013) Evolutionary consequences, constraints and potential of polyploidy in plants. *Cytogenetic and Genome Research* **140**:137–150.

Wickham H. (2016) *ggplot2: Elegant Graphics for Data Analysis*. Springer-Verlag, New York.

Šlenker M, Koutecký P, Marhold K. (2022) MorphoTools2: an R package for multivariate morphometric analysis. *Bioinformatics* **38**:2954–2955.

Strid A. (2016) Atlas of the Aegean Flora. Part 1: Text & Plates. Part 2: Maps. Englera 33. Botanic Garden and Botanical Museum Berlin, Freie Universität Berlin, Berlin, Germany.

Youssef S, Mahmood A, Cartereau M, Vela E. (2018) New cytological, morphological, and chorological data on *Prospero seisumsianum* (Rukšans & Zetterl.) Yıldırım (Asparagaceae) from the Zagros area. *Turkish Journal of Botany* **42**: Article 4.

Abstract

The Mediterranean *Prospero autumnale* complex (Asparagaceae) represents a cytologically diverse plant group, with at least four basic diploid cytotypes based on $x = 5$, 6 or 7. In addition to dysploidy, also auto- and allopolyploidy as well as the frequent presence of B chromosomes and supernumerary chromosomal segments contribute to its chromosomal diversification. Extensive cytogenetic analyses allowed for characterization of main diploid cytotypes and polyploid chromosomal races. Two of the diploid cytotypes co-occur on the island of Crete (B^6B^6, $2n = 2x = 12$; B^7B^7 $2n = 2x = 14$) and have given rise to four established and genomically distinct allotetraploid $B^6B^6B^7B^7$ cytotypes (Groups I-IV). The structured chromosomal variation has not, however, been mirrored by consistent morphological differentiation. In the light of this structured genomic variation, this study aimed to reanalyze the specific status of six previously described species of the complex endemic to the island of Crete (*P. depressum*, *P. minimum*, *P. rhadamanthi*, *P. idaeum*, *P. battagliae*, *P. hierapytnense*). Morphological, cytogenetic, and phylogenetic analyses were conducted on multiple plants collected from the type localities of these species. All populations were cytologically uniform and corresponded to previously described cytotypes, but their morphological characteristics overlapped considerably, failing to provide support for the recognition of the six Cretan *Prospero* species as taxonomically distinct. This precluded their clear morphological separation, especially when compared to the diversity within the complex. Phylogenetic analysis of nrITS sequences failed to recover these species as distinct lineages, instead supporting the integration of the individuals from the analysed populations into existing cytotypes. Instead, this study highlights the need for broader-scale sampling and combined cytogenetic, ecological, morphological, and genome-wide genomic analyses for better understanding of the patterns and processes underlying the morphological differentiation and perhaps speciation observed within the *Prospero autumnale* complex on Crete, as well as in the whole distribution range. Such analyses will serve as basis for future taxonomic revisions and inferences in the complex.

Zussamenfassung

Der mediterrane *Prospero autumnale*-Komplex (Asparagaceae) stellt eine zytologisch vielfältige Pflanzengruppe dar, die mindestens vier diploide Grundzytotypen auf der Basis von $x = 5$, 6 oder 7 aufweist. Neben Dysploidie tragen auch Auto- und Allopolyploidie sowie das häufige Vorhandensein von B-Chromosomen und zusätzlichen Chromosomensegmenten zur chromosomalen Diversifizierung bei. Umfassende zytogenetische Analysen ermöglichten die Charakterisierung der wichtigsten diploiden und polyploiden Zytotypen. Zwei der diploiden Zytotypen kommen gemeinsam auf der Insel Kreta vor (B^6B^6, $2n = 2x = 12$; B^7B^7, $2n = 2x = 14$) und haben durch Kreuzungen vier etablierte und genomisch unterschiedliche allotetraploide $B^6B^6B^7B^7$-Zytotypen (Gruppen I–IV) gebildet. Die strukturierte chromosomale Variation wird jedoch nicht von einer konsistenten morphologischen Differenzierung begleitet. Das Ziel dieser Studie war es, den spezifischen Status von sechs bereits zuvor beschriebenen Arten, die auf der Insel Kreta endemisch sind (*P. depressum*, *P. minimum*, *P. rhadamanthi*, *P. idaeum*, *P. battagliae*, P. *hierapytnense*), in Anbetracht der strukturierten genomischen Variation neu zu analysieren. Morphologische, zytogenetische und phylogenetische Analysen wurden an mehreren Pflanzen, die an den Typusorten dieser Arten gesammelt wurden durchgeführt. Alle Populationen waren zytologisch einheitlich und entsprachen den zuvor beschriebenen Zytotypen, aber ihre morphologischen Merkmale überschnitten sich deutlich,. Dies schloss bereits eine klare morphologische Trennung aus, insbesondere im Vergleich zur bestehendenVielfalt innerhalb des Komplexes. Die phylogenetische Analyse der nrITS Sequenzen liefertekeinen Hinweis, dass diese Arten eigenständige Linien seien, und unterstützte stattdessen die Integration der Individuen aus den untersuchten Populationen in bestehende Zytotypen. Diese Studie unterstreicht die Notwendigkeit umfangreicherer Probensammlungen und die Kombination zytogenetischer, ökologischer, morphologischer und genomweiter genomischer Analysen, um die Muster und Prozesse, die der morphologischen Differenzierung und möglicherweise der Artbildung innerhalb des *Prospero autumnale* Komplexes auf Kreta sowie im gesamten Verbreitungsgebiet zugrunde liegen besser zu verstehen. Solche Analysen werden als Grundlage für künftige taxonomische Überarbeitungen und Schlussfolgerungen in diesem Komplex dienen.